THE INVESTIGATIONS OF THE EFFECT OF IN-VITRO COMBINATION TREATMENT: CURCUMIN, ASPIRIN, AND SULFORAPHANE ON IDIOPATHIC PULMONARY FIBROSIS

by

Sarah Bui

A Thesis
Submitted to the
Graduate Faculty
of
George Mason University
in Partial Fulfillment of
The Requirements for the Degree
of
Master of Science
Biology

Committee:

_____	Dr. Geraldine Grant, Thesis Director
_____	Dr. Aarthi Narayanan, Committee Member
_____	Dr. Mikell Paige, Committee Member
_____	Dr. Geraldine Grant, Committee Member
_____	Dr. James D. Willett, Director, School of Systems Biology
_____	Dr. Donna M. Fox, Associate Dean, Office of Student Affairs & Special Programs, College of Science
_____	Dr. Peggy Agouris, Dean, College of Science
Date: _____	Spring Semester 2016 George Mason University, Fairfax, VA

The Investigations of the Effect of In-Vitro Combination Treatment: Curcumin, Aspirin, and Sulforaphane on Idiopathic Pulmonary Fibrosis

A Thesis submitted in partial fulfillment of the requirements for the degree of Master of Science at George Mason University

by

Sarah Bui
Bachelors of Science
Virginia Commonwealth University, 2013

Director: Geraldine Grant, Associate Professor
Department of Biology

Spring Semester 2016
George Mason University
Fairfax, VA

DEDICATION

This is dedicated to the people whose lives were changed because of Idiopathic Pulmonary Fibrosis.

ACKNOWLEDGEMENTS

I would like to thank my thesis director, Dr. Geraldine Grant, for her immense support and guidance. I am grateful for all the learning opportunities her mentorship has afforded me. I would like to express my gratitude to Dr. Aarthi Narayanan, my committee member, for her encouragement and tutelage during both semesters of graduate school. I would like to thank Dr. Mikell Paige, my committee member, for the generous support and interest in my project. I am thankful for all my lab mates, particularly Mrs. Eileen Liberti and Ms. Brenna Cannon for their assistance in the lab during the summer months. I am especially thankful for the genuine camaraderie of Mr. Luis Rodriguez, who fosters team spirit in our lab through his sharing of advice and resources. I would like to thank Dr. Steven Nathan and his entire team for their collaboration with our lab. This research would not be possible without the donors who contribute to science by providing our lab with research specimens. This research was funded by the Catherine and Bill Goodrum Lung Fund at Fairfax Inova Hospital. I would like to acknowledge Mrs. Catherine Goodrum, Mrs. Valerie Salentine, Mr. Bill Boyer, Mr. Pieter van den Assum, Pulmonary Fibrosis Events, and the Pulmonary Fibrosis Support Group of Greater Washington DC for inspiring me to continue my graduate studies and pulmonary fibrosis research. Lastly, a thank you to my mom and dad for their unwavering support and unconditional love. I am humbled by all the wonderful people I have had the privilege to meet throughout this process of graduate school, and it would not have been possible without them.

TABLE OF CONTENTS

LIST OF TABLES

LIST OF FIGURES

LIST OF ABBREVIATIONS

A549.....adenocarcinomic human alveolar basal epithelial cells
AEC.....Activated epithelial cell
AKT.....Protein kinase B
alpha-SMA.....alpha-smooth muscle actin
ASA.....Aspirin
Bcl2..... B-Cell CLL/Lymphoma 2
Bcl-xL.....B-cell lymphoma-extra large
CAS.....CAS
COLA1.....Collagen A1
CUR.....Curcumin
DISC..... Death-inducing signaling complex
DMEM.....Dulbecco's Modified Eagle Medium
ECM..... Extra cellular matrix
EMT.....Epithelial-to-mesenchymal transition
ERK.....Extracellular signal-regulated kinase
FADD.....Fas-Associated protein with Death Domain
FBS .....Fetal bovine serum
GSK3.....Glycogen synthase kinase 3
IAP..... Inhibitor of apoptotis proteins
IKβ.....Inhibitor of nuclear factor kappa-B kinase subunit beta
ILD..... Interstitial lung disease
ICC..... Immunocytochemistry
IPF.....Idiopathic pulmonary fibrosis
IPF-F.....Idiopathic pulmonary fibrosis fibroblasts
MET..... Mesenchymal-to-epithelial transition
MOMP..... mitochondrial outer membrane permeabilization
N-F.....Normal fibroblasts
NFKβ.....Nuclear Factor Kappa Beta
NRF2..... Nuclear factor (erythroid-derived 2)-like 2
PAI.....Plasminogen Activator Inhibitor
PARP.....Poly ADP ribose polymerase
PDGF .....Platelet-derived growth factor
Q-RTPCR..... Quantitative-real time polymerase chain reaction
SERCA.....sarcoendoplasmic reticulum (SR) calcium transport ATPase
SFN.....Sulforaphane
TBS .....Tris-buffered saline

TGF-β..... Transforming growth factor beta
TNF-alpha ..... Tumor necrosis factor-alpha
TUNEL.....deoxynucleotidyl transferase dUTP nick end labelling

ABSTRACT

THE INVESTIGATIONS OF THE EFFECT OF IN-VITRO COMBINATION TREATMENT: CURCUMIN, ASPIRIN, AND SULFORAPHANE ON IDIOPATHIC PULMONARY FIBROSIS

Sarah Bui, M.S.

George Mason University, 2016

Thesis Director: Dr. Geraldine Grant

Idiopathic Pulmonary Fibrosis (IPF) is a fatal interstitial lung disease characterized by an abundance of activated fibroblasts, which deposits excessive scar tissue in the lung. IPF is believed to be a result of an aberrant wound healing process in which fibroblasts are activated, undergo proliferation, and promote the excessive deposition of extracellular matrix. The source of injury to the alveolar epithelia which triggers this repair is unknown, however as a result of this aberrant process the fibroblasts appear to assume an apoptotic resistant phenotype. Curcumin has been shown to have global anti-fibrotic and apoptotic properties; however its bioavailability limits its application as a therapeutic. We sought to enhance curcumin's anti-fibrotic properties via its combination with aspirin and sulforaphane (CAS) in IPF and normal derived primary human fibroblasts *in vitro.* In addition, we sought to reveal the mechanism of apoptosis induced by this combined therapy. CAS enhanced anti-fibrotic properties were

demonstrated through the inhibition of fibroblast activation markers collagen A1 and smooth muscle actin. CAS exposure resulted in a significant increase in cell death, 73.97±31.31% ($p=0.0474^*$) and 49.64 ±6.87% ($p=0.0021^*$) decrease in normal fibroblast (N-F) and IPF fibroblast (IPF-F) over 48 hours. CAS-induced cell death was Caspase 3/7 dependent and results in subsequent proteolytic cleavage of PARP. Previous studies have associated sulforaphane mediated apoptosis with the ERK-MEK pathway and curcumin via the NFκβ pathway. Comparison of N-F and IPF-F mediate CAS cell death demonstrated a differential duration of ERK activation, sustained verses transient, which may be associated with N-F susceptibility to CAS and the apparent apoptotic resistance in IPF-F. NFκβ pathway proteins such as BclXL, AKT, beta catenin were also differentially regulated between IPF-F and N-F. The CAS combinatorial challenge demonstrated an effective apoptotic response in the cell lines. The contrasting routes of apoptosis between IPF-F and its N-F seen here highlight a significance difference between these cells which may indicate a significant role in disease progression. A further understanding of the apoptotic mechanisms in IPF-F will identify cell specific targets for the directed elimination of IPF-F while preserving the integrity of N-F and epithelial populations in the IPF lung.

1. INTRODUCTION TO IDIOPATHIC PULMONARY FIBROSIS

Idiopathic Pulmonary Fibrosis (IPF) is a fatal interstitial lung disease characterized by an abundance of activated fibroblasts known as myofibroblasts. These myofibroblasts deposits excessive scar tissue predominantly the lower peripheral lung zones. Repeated micro-injuries, potentially from inhaled infiltrates, to the alveolar epithelium are believed to initiate an aberrant wound healing response which involves the myofibroblasts. As the lung continues to scar, pulmonary function rapidly decline leading to poor blood oxygenation and eventually death due to organ failure within 3-5 years of diagnosis. With limited pharmaceutical options available, lung transplantation is considered the only cure for this disease. However, this option is available to very few giving the age of the patients and the limited organ availability. Therefore approximately 40 percent of patients eventually die of respiratory failure without a lung transplant (Gross, 2001). At any given time there are approximately 200,000 diagnosed pulmonary fibrosis patients struggling to breathe nationwide and an estimated 48,000 additional new patients are diagnosed every year (PF Coalition, 2011). The low patient survival rate combined with the increasing prevalence of this disease and the limited potency of the two recently FDA approved drugs among the heterogeneous patient population - all point towards an urgent need for new therapeutics.

1.1 Diagnosis

An IPF patient will usually present with symptoms such as dyspnea and shortness of breath during periods of physical exertion. Upon chest auscultation, 80% of patients exhibit audible crackles that are best described as "velcro-like" at the bases of the lungs. In more advanced stages of the disease, the crackles can be heard in the upper lung zones. Patients may suffer from clubbing of the fingers, cyanosis, and peripheral edema (Gross, 2001). Other secondary symptoms may include general fatigue, muscle weakness, and weight loss. There are currently no diagnostic tests available to confirm IPF in a patient based on the aforementioned symptoms. Final diagnosis results only from elimination of other known causes of interstitial lung disease; domestic and occupational environmental exposures, connective tissue disease, and drug toxicity (Raghu, 2011) and the presence of honeycombing on a high-resolution computed tomography (HRCT), combined with an invasive lung biopsy.

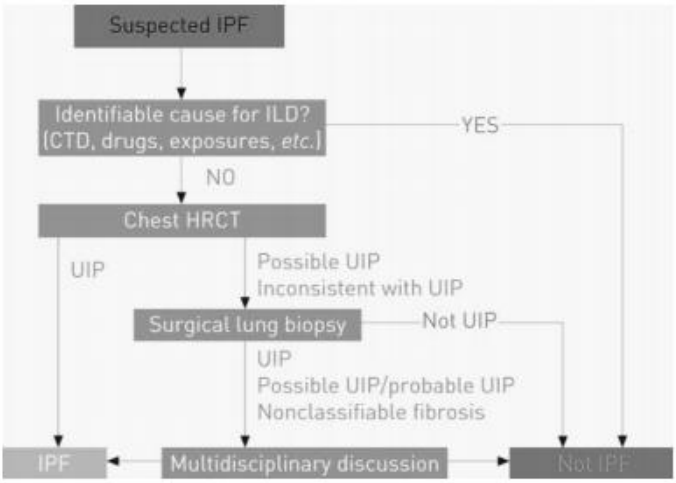

Figure I1. Diagnostic Algorithm for Idiopathic Pulmonary Fibrosis (Raghu, 2011).

Early diagnosis is challenging due to the absence of conclusive molecular biomarkers, however there is active research in predictive biomarkers for both familial and spontaneous IPF underway. Recently studies have indicated that circulating blood proteins such as matrix metalloproteinase 7 (MMP-7), Mucin-1 (MUC1 or KL-6), Surfactant Protein B (SFTPB1 or SP-A), Chemokine ligand 18 (CCL-18), or T-cell subpopulations may indicate distinct outcomes in certain patients with IPF. In a study performed by Rosas et al., a protein signature which included MMP-1, MMP-7, MMP-8, insulin like growth factor binding protein 1 (IGFBP-1) and Tumor Necrosis Factor Receptor Superfamily, Member 1A (TNFRSA1F) distinguished patients with IPF from control individuals with a sensitivity of 98.6% and a specificity of 98.1%. In addition, high blood concentrations of KL-6 (MUC-1), have been repeatedly shown to be predictive of decreased survival in IPF. Similarly, changes in circulating blood cell populations have been associated with ultimate outcome. In a cohort of 51 patients, increased circulating fibrocyte numbers predicted poor prognosis (Moeller, 2009) and downregulation of surface differentiation marker CD28 in circulating CD4 T cells was a marker of poor prognoses in a cohort of 89 IPF patients (Gilani, 2010). The power of these studies was limited by their size and replicative power however they underline the importance of a personalized medicine approach essential to the diagnosis, design of drug studies, and treatment of a heterogeneous IPF patient population.

1.2 Prognosis

The mean age for diagnosed IPF patients is 60.6, with a survival rate of only 3-5 years. There is higher prevalence within the male population; however, the reason for this

is unknown. The presentation of this disease is very heterogeneous with some patients progressing slowly while others are rapid progressors and require lung transplantation. In 2014, the FDA approved two drugs for the treatment of IPF, Nintendanib and Pirfenidone, may increase survival in non-advanced IPF by slowing the disease progression. Patients with a reduced full vital capacity (FVC) are more likely to have active alveolitis and are more likely to improve with treatment (Van Oortegem, 1994) but they are also more likely to have reduced survival. Other factors that have shown inconsistent or conflicting associations with progression and survival in IPF include male sex, age at diagnosis, smoking status, and duration of symptoms prior to diagnosis (Mapel, 1998).

1.3 Medical need

Repeated micro-injuries to the lung epithelium is believed to trigger Idiopathic Pulmonary Fibrosis. There is a strong correlation in disease incidence and environmental exposure to irritants. There have been reported cases of returning veterans suffering from lung symptoms similar to IPF, when upon biopsy of the lung tissue revealed the presence of titanium, magnesium, and iron. Suspected causes are environmental exposures to garbage burn pits, dust storms, industrial emissions and fires. Many military personnel are subject to potentially harmful particulates that increase their risk of developing IPF. Over 2 million United States men and women have been deployed to Iraq and Afghanistan since 2001 and according to one study published in the Journal of Occupational and Environmental Medicine, fourteen percent of the veterans returned with some sort of lung complication (Rose, 2012).

In years prior, illness associated with being in the region was called Gulf War Syndrome and included progressive dsypnea. There were 5.2 million who served during the Gulf War Era, representing the military population of the last 25 years. Gulf War troops were primarily exposed to DEET, organophosphate pesticides, and permethrin. They also inhaled smoke from 600 oil wells that were ignited by the Iraqi army for 5 consecutive months in 1991. Among the first 20,000 Department of Defense Comprehensive Clinical Evaluation Program (CCEP) participants, there were 14 (0.07%) with confirmed interstitial pulmonary fibrosis (Joseph, 1997).

Between 60,000 to 70,000 responders were exposed to the dust that clouded Manhattan and parts of Brooklyn, New York after the attack on the World Trade Center on September 11, 2001 (Wu, 2010). The WTC dust contained airborne pollutants such as silicates, aluminum, magnesium, calcium sulfate and calcium phosphate. The healthy responders during clean up and recovery at the crash site reported respiratory impairment in the years that followed, and some were later diagnosed with interstitial lung disease (Wu, 2010).

An average of 40,000 people die in the U.S. every year from IPF. People age 65 years and older are at higher risk of developing IPF (Raghu, 2006). This population also happens to be the same age as many of the retired veterans. There are 21.8 million veterans of the U.S. armed forces as of 2014, according the Census Bureau, approximately 10 percent of whom are women. IPF affects more men than women, meaning 19.6 million men in the veteran population are at a greater risk of being diagnosed with IPF.

In the United States estimated prevalence of IPF ranges from 14 to 42.7 cases and incidence ranges from 6.8 to 16.3 cases per 100,000 persons (Raghu, 2006). With the steady advancing mean age of the U.S. population, the incidence and prevalence of IPF is likely to continue to rise in the future. However common malignancies attract more research resources, although IPF appears to be approximately just as prevalent and fatal a disease (Well, 2007).

Our research could further the understanding of the mechanisms of IPF and identify stimuli that occurs during pulmonary injury which propagates the fibrotic response. Uncovering cell specific targets will allow for the elimination of the IPF deregulated fibroblasts while preserving of the integrity of the normal fibroblast and epithelial populations in the IPF lung. Development of such potential therapeutics which target only the IPF fibroblast population will allow for improved quality of life.

1.4 Treatment

Currently there are only 2 course of treatment for IPF, 1: Lung transplant or 2: Nintendanib or Pirfenidone, two recently FDA approved therapies which work on a small percentage of the IPF population.

The medications, Nintendanib and Pirfenidone, slow the progression of IPF by acting on multiple pathways involved in lung scarring. The exact mechanisms of the drugs have yet to be determined and their efficacy is limited in the heterogeneous IPF population. Therefore, by investigating the mechanisms of apoptosis in IPF derived human fibroblasts, the behavior of these cells could be manipulated for a desirable outcome such as the programmed cell death of the rogue fibroblasts or the inhibition of

profibrotic cytokines through blocking of a pathway that is differentially activated in fibroblasts at the fibrotic foci.

1.4.1 Traditional therapy

Traditionally, the assumption was that IPF is a chronic, unresolved inflammatory disease. Corticosteroids in combination with immunosuppressants such as azathioprine or cyclophosphamide have been prescribed to IPF patients for decades (Selman, 2002). It was reported that fifteen to thirty percent of patients on corticosteroids alone improved physiologically or radiographically (Thannickal, 2005). However, that study is now believed by researchers to have included patients with nonspecific interstitial pneumonia (NSIP), respiratory bronchiolitis-associated interstitial lung disease, or cryptogenic organizing pneumonia, which are all responsive to steroid treatment (Walter, 2006). IPF patients on corticosteroids with or without immunosuppressive drugs experienced adverse toxic effects or observed no benefit (Selman, 2002). The randomized, double-blind, placebo-controlled PANTHER trial assigned patients with idiopathic pulmonary fibrosis who had mild-to-moderate lung-function impairment to one of three groups — receiving a combination of prednisone, azathioprine, and N-acetylcystine (NAC) (combination therapy), NAC alone, or placebo. After 32 weeks, all arms except for NAC alone and the placebo were terminated due to an increased rate of death (8 vs. 1, $P=0.01$) and hospitalization (23 vs. 7, $P<0.001$). Another study added cylcophosphamide to the regimen of IPF patients who did not respond to corticosteroids and again, demonstrated anti-inflammatory and immunosuppressive therapies did not improve the quality of life or survival rate of IPF patients (Zisman, 2000). These observations, coupled with no

evidence of physiological or clinical benefit suggests inflammation is not a involved in the pathogenesis of IPF. Furthermore, concurrent with the inefficacies of steroidal treatments is the lack of inflammatory cells in the lung pathology of IPF patients (Bringardener, 2008). Current data suggest that the pathophysiology of the disease is more a product of fibroblast dysfunction than of dysregulated inflammation (Willis, 2006). Additionally, new insights into the disease, like identifying genetic polymorphisms in genes regulating telomere length, and mitochondrial metabolism of reactive oxygen species suggest the dominant role of fibroblast dysfunction resulting in a process of dysregulated tissue repair in IPF, as opposed to an inflammatory process.

1.4.2 Current therapeutic approaches

Antifibrotic drugs and anticytokine agents are promising avenues of drug research for IPF treatment because of the paradigm shift from characterizing IPF as an inflammatory disease to a progressive fibrotic disease. Some major antifibrotic and anticytokine agents that are of research interest for potential treatment of IPF include: colchicine, penicillamine, rapamycin, etanercept, transforming growth factor-β (TGF-β) antagonist (Bouros, 2005). Anticytokine therapeutics capable of abrogating the activation of lung fibroblasts may control the progression of IPF and improve respiratory functions. Furthermore, the antifibrotic treatments can modulate the process of dysregulated tissue repair involved in the pathogenesis of IPF.

1.4.3 Pirfenidone

Pirfenidone is indicated for the treatment of mild to moderate IPF. While its mechanism is not well understood, it has anti-inflammatory properties and is anti-fibrotic by inhibiting collagen production and reduces the production of fibroogenic mediators.

Pirfenidone was part of the ASCEND and CAPACITY randomized double-blind placebo trials which. suggested reduced disease progression, as reflected by lung function, exercise tolerance, and progression-free survival. It was reported that patients who failed conventional therapy appeared to stabilize lung function after 6 months of treatment with pirfenidone. In a trial of 107 IPF patients, the drug demonstrated a slight efficacy in protecting patients against acute exacerbations and slowed decline in FVC at 9 months (Azuma, 2005). In an open-label, pilot study of 800mg three times/day, patients who had completed radiation therapy and developed fibrosis as a result were given pirfenidone. These patients reported improved respiratory functions and stabilized symptomology (Simone, 2007). Adverse side effects of the drug varied among patients, but the most common were photosensitivity, fatigue, abdominal discomfort, and loss of appetite. Photosensitivity reactions have resulted in rash, pruritus and/or dry skin. Patients are usually instructed to use sunscreen and to wear protective clothing. The FDA approved pirfenidone for treatment of IPF in October 2015. In the same year, a second drug was also approved by the FDA: Nintendanib.

1.4.4 Nintendanib

Nintendanib is a small molecule tyrosine-kinase inhibitor and targets vascular endothelial growth factor receptor (VEGFR), fibroblast growth factor rector (FGFR) and

platlet derived growth factor receptor (PDGFR), all of which are believed to play a role in IPF. It was developed by Boehringer Ingelheim and is marketed under the brand names Ofev and Vargatef. The route of administration can be through oral or intravenous. The biological half-life of the drug is 10-15 hours and has a bioavailability of 4.7%.

Nintendanib has limited efficacy in the heterogeneous patient population and is contraindicated for patients with liver disease, as the drug is metabolized in the liver. Patients who benefitted from the drug observed a slower decrease in FVC. Patients noted side effects such as nausea, vomiting, and diarrhea after taking Nintendanib. Interestingly, although it is an angiogenesis inhibitor, complications to wound healing has not been reported in the IPF population treated with the drug.

1.5 Fibroblasts in IPF Pathogenesis

IPF is believed to be a result of an aberrant wound healing process in which fibroblasts are activated, undergo proliferation, and promote the excessive deposition of extracellular matrix (ECM). The source of injury to the alveolar epithelia which triggers this repair is unknown, however as a result of this aberrant process the fibroblasts appear become resistant to apoptosis.

The histopathological features of Idiopathic Pulmonary Fibrosis when observed through computed tomographic (CT) scans include the presence of honeycombing patterns indicative of chronic scarring and areas of acute lung injury with fibrotic foci (Gross, 2001). The fibrotic zones are characterized by an abundance of vigorously proliferating fibroblasts expressing alpha-smooth muscle actin; resulting in excessive collagen deposition and distortion of normal lung parenchyma architecture through the

remodeling of the extracellular matrix (ECM). During the normal wound healing process, activated fibroblasts will undergo apoptosis after repairing an injury. However, it has been postulated that fibroblasts in IPF are more resistant to programmed cell death which leads to decreased senescence, prolonged fibroblast survival, elevated secretion of autocrine growth factors, enhanced collagen synthesis and ultimately, disease progression (Moore, 2013).

In IPF, fibrosis of the lungs begins at the fibrotic foci where myofibroblasts are over-active. In previous cancer studies, MMPs have been shown to enhance cell proliferation through proteolysis of insulin-like growth factor binding protein, resulting in increased bioavailability of insulin-like growth factors and thereby stimulating cell growth. MMP-7, also known as matrilysin, is associated with tumorigenesis and cancer progression but also a current prognostic biomarker of interest for IPF (Sokai, 2015). MMP-7 converts E-cadherin to soluble E-cadherin to promote cell invasion. Furthermore, MMP-7 can cleave tumor necrosis factor (TNF)-alpha precursor to release soluble TNF-alpha and increase apoptosis in the alveolar lung epithelial cell populations, propagating the aberrant wound healing process in IPF (Richards, 2012).

Alveolar epithelial cells (AECs) can acquire a mesenchymal phenotype through a process known as epithelial-mesenchymal transition (EMT), and may serve as an important source of fibroblasts and myofibroblasts (Willis, 2006). However, emerging evidence suggests the myofibroblasts can arise from fibroblasts residing in the adventita of perivascular and peribronchial tissue. In addition, myofibroblasts has also been hypothesized to be derived from fibrocytes circulating in the blood and bone marrow

derived progenitor cells (Hashimoto, 2004; Dunsmore, 2004; Phillips, 2004). Injury to AECs combined with parachymal cell and alveolar epithelial cell death are observed in experimental animal models of lung injury and patients with IPF. The formation of gaps in the epithelial basement membrane due the apoptosis and cellular insult promotes the migration of fibroblasts through these gaps into the alveolar space. The interstitial fibrosis and subsequent intra-alveolar fibrosis result in ECM remodeling and progression of IPF (Uhal, 19998; Bardales, 1996). Therefore, major therapeutic strategies for IPF is to control the activation of myofibroblasts, migration of fibroblasts, and prevent the apoptosis of the epithelial cells while inducing regulated cell death of diseased fibroblasts.

1.6 Apoptosis overview

Apoptotic Morphology

During apoptosis, a process of regulated cell death, the cell undergoes changes in morphology. First, the cell shrinks and the chromatin condenses. The cell membrane then begins to show blebs or spikes, depending on the cell type (Fuchs, 2011). These protrusions, or apoptotic bodies, eventually separate from the dying cell and are phagocytosed by macrophages and other proximal cells. The mitochondria also undergo changes as it loses its electrochemical gradient of the outer membrane and the integrity of the membrane is compromised (Pradelli, 2010). The formation of pores in the mitochondrial outer membrane (MOM) can lead to pro-apoptotic leakage of cytochrome c into the cytoplasm. The apoptotic cell does not stimulate an inflammatory response, in contrast to a necrotic cell. Necrosis is a process of overwhelming cell death, which is first

marked by a loss of cell membrane integrity, followed by the swelling of the mitochondria and the cell (Degterev, 2008). Eventually, the swelling culminates into the lysis of the cell and many of its internal organelles. There is no apoptotic body formation and the dying cell triggers the inflammatory and pro-apoptotic response of neighboring cells.

Apoptosis and necrosis represent two extremes of a continuum of cell death. This continuum includes many variations. For example, paraptosis is a process of cell death that requires gene expression but morphology does not resemble apoptosis or necrosis (Sperandio, 2000). To further illustrate the diversity of cell death mechanisms, secondary necrosis is a term used to describe the death of cells cultured *in vitro* after an extended period of incubation (Van Breda, 2008). Because cell death has many different pathways leading to the same outcome, examination of biochemical markers at selected time points is important to determining the mechanism of cell death.

Molecular Players in Apoptosis

Caspases are constitutively expressed in most cell types. Their structure consists of several domains: N-terminal prodomain, a large subunit, and a small subunit. Proteolytic cleavage of the caspase at a specific aspartic acid between the small and large subunits and removal of the prodomain results in activation of the caspase (Pradelli, 2010). The active caspase protein is a tetramer formed by two heterodimers of one large and one small subunit. Human caspase-8 and caspase-9 are known as “initiator caspases” because they are capable of activating “effector caspases” such as caspase-3. Active

caspase-3 cleaves downstream targets such as DNA repair enzymes and irreversibly commits the cell to the apoptotic fate (Kurokawa, 2009).

Bcl-2 family proteins are classified as pro-apoptotic or anti-apoptotic. The pro-apoptotic members of the Bcl-2 family- Bid, Bad, Bax, play a role in mitochondrial outer membrane permeabilization (MOMP) (Kaufmann, 2012). During MOMP, cytochrome c and Smac/Diablo is released from the mitochondria into the cytosol. Cytochrome c binds to Apaf-1 and dATP, to form a complex with pro-caspase 9 known as the apoptosome. This protein complex then activates caspase 3 and deactivates inhibitor of apoptosis proteins (IAPs). However, some intrinsic apoptotic pathways are cytochrome c independent (Pradelli, 2010). These apoptotic pathways rely on signals from the endoplasmic reticulum (ER) induced by stressors such as accumulation of folded or malfolded proteins triggered by hypoxia, a lack in nutrients, or over-expression of some proteins.

In the extrinsic apoptotic pathway, a ligand on the cell surface is activated and initiates a signaling cascade to trigger apoptosis. As an example, Fas-dependent activation of the death receptor pathway relies on the aggregation and conformational change of activated Fas receptors which initiates the assembly of death inducing signaling complex (DISC). DISC is comprised of the Fas receptors, Fas Ligand (FasL) and Fas associated death domain protein (FADD). The adaptor protein, FADD, recruits procaspase-8 that activates and cleaves effector caspases 3, 6, and 7 (Wang, 2001). In some cells, activation of caspase-8 can lead to the cleavage of Bcl-2 protein family

member, Bid. Upon Bid cleavage, Bax-mediated release of cytochrome c from the mitochondria further committing the cell to undergo apoptosis.

The anti-apoptotic Bcl-2 protein family members, Bcl-2 and Bcl-XL, protect the cells from apoptosis by sequestering pro-apoptotic proteins or inhibiting their activity. The activity of these proteins are regulated by proteolytic processing, phosphorylation, and sequestration. Depending on the balance of activated pro-apoptotic or anti-apoptotic proteins, the cell may die or survive.

1.7 Targeting fibroblasts for apoptosis

Thakkar et al. have demonstrated that curcumin, aspirin, and sulforaphane (CAS) combinatorial therapy inhibits pancreatic cancer cell growth by inducing apoptosis and proposed the sustain activation of ERK 1/2 with the down-regulation of NF-kappaB pathway as possible mechanisms (Thakkar, 2013). Nanoencapsulated (solid lipid nanoparticles; SLN) of the CAS therapeutic suppressed pancreatic cancer neoplastic lesions in a golden hamster model was a proof-of-concept for the use of low-dose, nanotechnology based combinatorial regimen for drug therapeutics (Grandhi, 2013). Using the same approach as Thakkar et al., we hoped to suppress fibrosis in the IPF lung through CAS-induced apoptosis of fibroblasts and ultimately move on to *in vivo* testing with a bleomycin model of IPF.

1.7.1 Curcumin

Curcumin is a natural compound isolated from *Curcuma longa*, commonly known as turmeric. Previous studies have demonstrated the anti-fibrotic properties of curcumin,

mainly through its ability to modulate survival pathways, trigger cell cycle arrest, and induce apoptosis in lung and liver fibrosis models (Lin, 2009; Zhang, 2011; Smith, 2010; Chen, 2008). A study has shown that 104 out of 214 apoptosis-associated genes were altered after curcumin treatment in human breast cancer and mammary epithelial cell lines. (Ramachandran, 2005). Although the precise molecular targets of curcumin are unknown due to the results often being cell type specific or dosage dependent, the overwhelming number of apoptotic genes affected by curcumin suggests it is involved in multiple complex pathways. Curcumin modulates the growth of cells, mostly tumor cells, through regulation of cell proliferation pathways (cyclin D1, c-myc), cell survival pathways (NFKβ, Bcl-2, Bcl-xL, XIAP, c-IAP1), caspase activation pathways (caspase-3,8,9, mitochondrial pathways, and protein kinase pathways (Akt, MAPK) (Ravindran, 2009).

1.7.2 Aspirin

Aspirin (ASA) is a non-steroidal anti-inflammatory drug (NSAID) used in many chemotherapeutics due to its antineoplastic and anti-angiogenic properties. Aspirin has been associated with inhibition of cyclooxygenase (COX) enzymes COX -1 and COX-2. Studies demonstrated COX-2 expression stimulates VEGF production, which is associated with tumor progression. IPF fibroblasts are similarly activated by growth factors causing an overabundant myofibroblast population in the diseased lung. Cox-2 inhibitors such as Celecoxib were clinically tested for usage colorectal adenoma treatment. Borthwick et al. demonstrated that aspirin can work through a novel mechanism independent of Cox by directly inhibiting endothelial cell proliferation. At 2-

5mM aspirin, there was a significant decrease in cell viability after 48 hours. However a Cox-1 or Cox-2 inhibitor did not have an effect on cell proliferation or cell viability. Based on these results, the authors concluded the mechanism of action for aspirin on endothelial cell apoptosis is independent of Cox and potentially mediated by activation of nuclear factor kappa-B. More recent studies have similarly shown that aspirin can activate NFKβ signaling and induce apoptosis in colorectal cancer cell lines (Stark, 2001). Stark et al concluded that aspirin-induced apoptosis in colon cancer cells was mediated by a reduction in cytoplasmic IKβα that was due to a phosphorylation-dependent proteasome-mediated degradation of the protein. Once translocation of NFKβ was inhibited by generating cell lines with an active super-repressor IKβα, the cells abrogated aspirin-induced apoptosis. Therefore the authors concluded activation of the NFKβ pathway is a novel mechanism for aspirin-induced apoptosis.

1.7.3 Sulforaphane

Sulforaphane (SFN) is an isothiocyanate found in cruciferous vegetables. Crucifers are part of the Brassicaceae family and include *Brassica oleracea* (broccoli, cabbage, cauliflower, brussel sprouts), *B. rapa* (Chinese cabbage and turnips) watercress, and rocket. The consumption of cruciferous vegetables has been linked to lowering risks of cancer in the prostate (Giovannucci, 2003), lungs (Spitz, 2000; Wang, 2004; London 2000; Zhao, 2001), breasts (Ambrosone, 2004; Fowke, 2003), and colon (Seow,2001). Sulforaphane has antioxidant properties which has potential to mediate the pathogenesis of IPF through regulating the amount of reactive oxygen species in the alveolar environment.

Glutathione (GSH) is an important protective antioxidant against free radicals. Neutrophils from the lungs of patients with IPF generate higher concentrations of oxidants in association with high concentrations of myeloperoxidase and lower concentrations of GSH (Cantin, 1987; Cantin, 1989). Exposure of cells to isothiocyanates (ITCs) leads to an increase of –SH groups which sensitizes the cells to oxidative stress and stress-induced damage. As ITCs accumulate in the cells, it binds with intracellular thiols like GSH which function as buffer systems in the cell to maintain an oxidation-reduction balance in the cell and protect it from reactive oxygen species. With the loss of GSH, the cell becomes more susceptible to oxidative stress. A state of increased oxidative stress with increased release of oxidants from neutrophils, macrophages, and fibroblasts and decreased levels of antioxidants has been hypothesized to contribute to the pathogenesis of IPF. An imbalance of reactive oxygen species and protective antioxidants may impair cellular functions. A hyperoxic environment may not be well-tolerated by cells in the IPF lung, inducing apoptosis and contributing to the pathogenesis of the disease.

Sulforaphane is also able to activate the intrinsic apoptotic pathway, through cytochrome c release and activation of initiator caspase 9 and effector caspase 3. Furthermore, sulforaphane induced activation of caspase 12 from ER stress also initiates pro-apoptotic pathways. MAPK cascades have three distinct pathways: extracellular signal-regulated kinase (ERK), c-Jun N-terminal kinase (JNK) and p38. The MAPK pathway activated by sulforaphane may induce apoptosis. In pancreatic cancer cells, ERK1/2 is implicated in cell death by CAS challenge (Thakkar, 2013). Sulforaphane

activated both ERK and p38 in PC-3 cells. HepG2 cells were up regulated in all three MAPK pathways with SFN exposure, but only JNK was activated in DU145 and HepG2-C8 cells. In prostate cancer cells, a study demonstrated sulforaphane can trigger cell death in a non-apoptotic manner independent of caspase activation. Sulforaphane reduced prostate cancer cell viability through autophagy and inhibition of cytochrome c release.

1.7.4 CAS combinatorial apoptotic challenge

The different mechanisms by which curcumin, aspirin, and sulforaphane can induce apoptosis is complex and the redundancy in the pathways can involve different effectors eventually converging on the same apoptotic signaling cascade. We sought to enhance curcumin's anti-fibrotic properties via its combination with aspirin and sulforaphane (CAS) in IPF and normal derived primary human fibroblasts *in vitro.* In addition, we sought to reveal the mechanism of apoptosis induced by this combined therapy.

2. METHODS

2.1 Materials

All chemicals and supplies were purchased from Fisher Scientific (Pittsburgh, PA) unless specified. Antibodies were purchased from Abcam (Cambridge, MA) and primers from Invitrogen (Carlsbad, CA). Curcumin was purchased from Alexis Biochemicals (San Diego, CA). Human lung fibroblasts MRC-5 (CCL-171) and lung epithelial cells A549 (CCL-185) were obtained from the American Type Culture Collection (ATCC, Manassas, VA).

Lung procurement

Lung samples (IPF and normal) were obtained from Inova Fairfax Hospital and the Washington Regional Transplant Community (WRTC) respectively, under approved investigative protocols (Inova Health System and George Mason University Institutional Review Boards).

Primary fibroblast isolation and culture

IPF-F and normal-F were isolated from lung tissue by enzymatic dissociation and differential binding, as described previously [19-24]. Fibroblasts were cultured in vitro ≤ 80% confluence and maintained within a 10 passage range in complete media (Dulbecco's Modified Eagle medium (DMEM, Invitrogen) supplemented with 10% Foetal Bovine Serum (FBS, Valley Biomedical, VA) and 10,00 units/mL of penicillin, 10,00 µg/mL of streptomycin, and 2.5 µg/mL of Fungizone® (PSF)).

2.2 Pretreatment of cells

Prior to each experiment, all cells were pretreated in the same manner. Specifically cells were grown to 90% confluence and serum-starved overnight. Cells were seeded the following day at 5000 cells per well in a 96 well plate, or $1x10^6$ cells for a $100mm^2$ dish, in complete media without PSF, and allowed to attach overnight (over 16-24 hours). Negative controls included cells in media and DMSO vehicle controls. After 48 hours, cells were flash frozen in liquid nitrogen and stored at -80o C for RNA and protein analysis.

2.3 Cell Viability Analysis

The effect of curcumin on IPF-F (n=3), normal-F (n=3), and A549 cell viability was determined over 48 hours at concentrations of 0, 5, 10, 20, 40, 60, and 80 µM curcumin dissolved in 0.1% DMSO, using the CellTiter-Glo® Luminescent Cell Viability Assay (Promega, Madison, WI).

2.4 Total RNA Extraction

Total RNA was extracted using the RNeasy® Kit (Qiagen) from treated and untreated control cells after 48 hours of CAS exposure. All RNA was quantified using a Nanodrop™ spectrophotometer (Nanodrop™ 3.0.0, Agilent Technologies) and stored at -80o C

2.5 QPCR

Gene Expression Analysis- ACTA2, COL1A1, Nrf2, and Cyclin D, was assessed by quantitative real time PCR (qPCR). Total RNA (1µg) was reverse transcribed to

cDNA using the iscript cDNA synthesis kit (BioRad). qPCR was carried out using Quantifast SYBR green PCR kit (Qiagen). All gene expressions were normalized to 18S gene expression using the Comparative Ct 2-(delta)(delta)Ct method (Pfaffl, 2001). The fold difference was calculated in comparison to cells exposed to CAS for 48 hours and cells not exposed to CAS. Gene expression was analyzed for: alpha-Smooth Muscle Actin (alpha-SMA) (ACTA2), Cyclin D1 (CCND1), Collagen 1A1 (COL1A).

18S forward primer: AGGAATTCCCAGTAAGTGCG

18S reverse primer: GCCTCACTAAACCATCCAA

ACTA2 forward primer: GTGTTGCCCCTGAAGAGCAT

ACTA2 reverse primer: GCTGGGACATTGAAAGTCTCA

COL 1A1 forward primer: GTCGAGGGCCAAGACGAAG

COL 1A1 reverse primer: CAGATCACGTCATCGCACAAC

Nrf2 forward primer: GAG AGC CCA GTC TTC ATT GC

Nrf2 reverse primer: TGC TCA ATG TCC GTG TGC AT

CCND1 forward primer: GTGCTGCGAAGTGGAAACC

CCND1 reverse primer: ATCCAGGTGGCGACGATCT

2.7 Total Protein Extraction

Total cellular protein was isolated using RIPA buffer (Pierce), with addition of complete mini protease inhibitor cocktail tablets (Roche) and PhosSTOP™ phosphatase inhibitors cocktail tablets (Roche) per the manufacturer's instructions. Lysed cells were centrifuged at 13,000Xg for 20 minutes to remove cellular debris. The resulting

supernatant was collected and stored at -80o C. Total protein concentration was determined by Bradford assay (Bio-Rad).

2.8 Western Blot

Western blot analysis- 20µg of total cellular protein was subjected to gel electrophoresis using a 4-12% Bis-Tris gradient gel (Invitrogen). Visible molecular weight markers were included (Dual Precision Plus Marker, Bio-Rad or Pre-Stained Protein Ladder, Fisher). Proteins were transferred to nitrocellulose membrane using the iBLOT® system (Invitrogen). All membranes were blocked with 5% non-fat dried milk in Tris-buffered saline (TBS) containing 0.1% Tween-20 (TBS-T) for 1 hour at room temperature. After blocking, the TBS-T was replaced with TBS-T 5% non-fat dried milk containing primary antibodies (Cell Signaling) at a concentration of 1µg/ml of each antibody overnight at 4o C. After overnight incubation each membrane was washed 5 times for 5 minutes (5x5mins) with TBS-T, followed by incubation with the appropriate horseradish peroxidase (HRP)-linked secondary antibodies in TBS-T 5% non-fat dried milk for 1 hour at room temperature. Afterward, each membrane was washed with TBS-T 5X5min then visualized by incubation with chemiluminescent Super Signal West Femto Max Sensitivity Substrate (Pierce). For normalization blots were then stripped using Restore Western Blot Stripping Buffer (Thermo Scientific) according to the manufacturer's protocol. Each membrane was then re-probed with a primary antibody and secondary antibody as previously described. All immune-blots were imaged using ChemiDoc™ XRS System (Bio-Rad) and densitometry analysis was performed using Quantity One software (Bio-Rad). Protein expression was normalized to beta actin (ab

8227, Abcam), COXIV (ab 4844, Cell Signaling), GAPDH (ab 5174, Cell Signaling) or beta tubulin (ab 2146, Cell Signaling) expression.

2.9 TUNEL Assay

Apoptosis was assessed using a deoxynucleotidyl transferase dUTP nick end labelling (TUNEL) assay (Roche). Cells were seeded onto chamber slides and treated with DMSO, CAS, 20uM CUR, or CAS and U0126 for 48 hours. The TUNEL assay was performed as directed by the manufacturer. Essentially the cells were fixed in 4% paraformaldehyde, washed in PBS, and permeabilized with 0.1% Triton X-100 in 0.1% sodium citrate for 2 minutes on ice. Cells were washed well in PBS before addition of 50ul TUNEL reaction mixture containing FTIC conjugated dUTP to each well and incubated for 1 hour at 37C in the dark. Slides were washed in PBS and mounted with Cytoseal aqueous mounting medium. Results were visualized using EVOS fluorescent microscope and apoptotic cells were counted in three field of view in each chamber.

2.10 ApoGLO Caspase3/7 Assay

Caspase-3/7 activity was measured using the Apo-ONE® Homogeneous Caspase-3/7 Assay (Promega). The caspase-3/7 substrate rhodamine 110, bis-(N-CBZL-aspartyl-L-glutamyl-L-valyl-L-aspartic acid amide; Z-DEVD-R110), exists as a profluorescent substrate prior to the assay. The buffer and substrate were mixed and added to a 96-well plate of cells after 48h of CAS challenge. Upon sequential cleavage and removal of the DEVD peptides by caspase-3/7 activity and excitation at 499nm, the rhodamine 110 leaving group becomes intensely fluorescent. The fluorescence was measured at 530nm.

2.11 Immunocytochemistry

IPF fibroblasts and normal fibroblasts were seeded, serum starved, and treated with CAS for 48 hours. The slides were fixed in 1.6% paraformaldehyde for 10 minutes at room temperature. Slides were then washed with PBS and permeabilized with (X-100) Triton X. Each slide was then blocked with 1% BSA in PBS for 2 hours at room temperature. Immunocytochemistry (ICC) was performed by incubation overnight at 4o C in the appropriate primary antibodies (Cell Signaling) diluted in PBS with 1% BSA concurrently. Primary antibodies raised in different species were used for double staining. Subsequent to primary incubation, slides were washed 3X5mins in PBS followed by incubation with species complimentary secondary antibodies conjugated with Alexa Fluor® for 1 hour at room temperature in the dark. Each slide was then washed 3X5mins in PBS. Nuclei were visualized by counter-staining with DAPI (1µg/ml in PBS) for 1 minute. Slides were then mounted in Cytoseal^{TM} XYL (Richard-Allan Scientific) and covered with a cover slip. Visualization was carried out using a EVOS Fluorescent microscope. Images were processed using Adobe Photoshop® Elements.

2.12 Microarray

RNA was extracted using a Qiagen RNeasy kit (Qiagen, Valencia, CA) and DNase was treated using DNase free (Ambion, Austin, TX). The quality and quantity of the RNA was determined using RNA 6000 nanochips and an Agilent Bioanalyzer. For microarray analysis, 1 µg of RNA was amplified and amino-allylated using the MessageAmp II aRNA kit (Ambion). All microarrays were carried out by the Duke Institute for Genome Sciences and Policy, Microarray Facility using HO36K human chip

representing 33,791 transcripts from the Ensembl Human Build (BI-35C) including 22,169 unique genes (Operon Human Oligo set V4), and two color amino-allylated amplified RNAs: cy5 patient and normal samples, and cy3 Stratagene human reference RNA.

2.13 Gene ontological analysis

Functional categories enriched in the differentially expressed genes were identified using the functional annotation and clustering tool of the Database for Annotation, Visualization, and Integrated Discovery (DAVID) as previously described[2]. The probability that a gene ontology (GO) biological process term is overrepresented is expressed by DAVID as an EASE score. Briefly this score is determined by a modified Fisher's exact test comparing the proportion of genes within the GO term that are represented in a supplied list of genes to the genes in the whole genome that are part of the same GO term. Clusters of overrepresentation are generated based on similarity of differentially expressed genes assigned to each GO term. The enrichment score is a minus log transformed geometric mean of the EASE scores of the constitutive terms. Each whole number point on the enrichment score represents a 10 fold decrease in EASE score, as an example an enrichment score or 3 represents and average EASE score of 0.001 for the cluster and a score of 4 corresponds to a 0.0001 average EASE score.

2.12 Statistical Analysis

Statistical analyses were carried out using Prism 3.03 software (GraphPad). Paired t-test was used for cell viability, proliferation, immunoblot, and TUNEL assays.

All data presented are representative of experiments performed at least in triplicate. A p-value of less than 0.05 was considered significant.

3. RESULTS

Project rationale and preliminary findings: The rationale for this project originated from previous data which highlights curcumin's antifibrotic capabilities in IPF and normal lung fibroblasts *in vitro* [Chhina, PhD Dissertation, GMU, 2010].

3.1 Curcumin preferentially inhibits cell viability of fibroblasts

Exposure to curcumin (40μM -100μM) significant inhibited cell viability. Specifically, 48-hour exposure to 40μM CUR reduced cell survival to 41.12±7.84% (P=0.027) in IPF-F (n=3), 48.08±1.78% (P=0.034) in Normal-F (n=3), while no significant effect was observed in A549 epithelial cells 62.56.12±3.26% (P=0.068) cell survival.

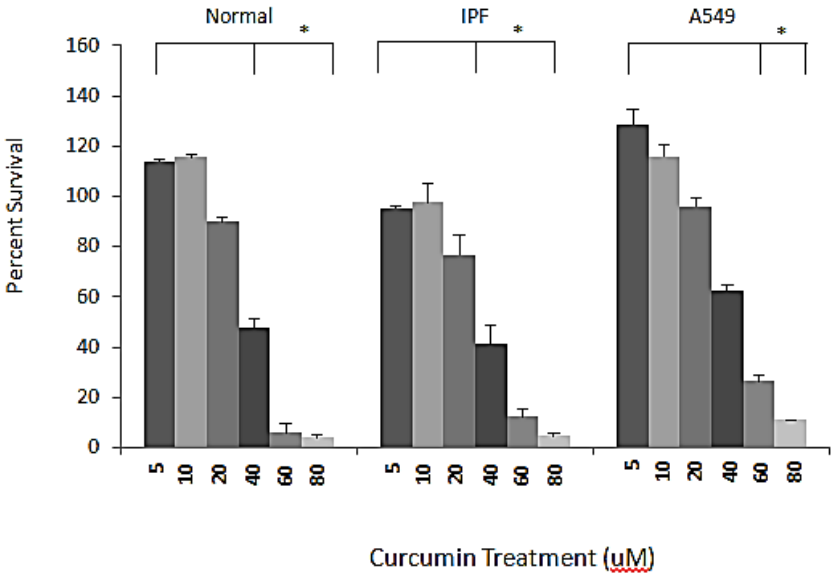

Figure 1. IPF-F, Normal-F and A549 cell survival in the presence of 0-80 μM curcumin over 48 hours. *P≤ 0.05; represents statistical significance between control and treatment groups as determined by paired t test.

3.2 Aspirin and sulforaphane synergistically potentiates curcumin's effect on the reduction of cell viability in combination treatment

To determine the effect of the combination of CUR, SFN and ASA each compound was tested individually to assess its dose-dependent inhibition of cell viability over 48 hour exposure. The concentrations of ASA, CUR, and SFN 3mM, 20μM, and 40μM, respectively we selected for further studies as these were the maximum concentrations individually that did not significant effect cell viability.

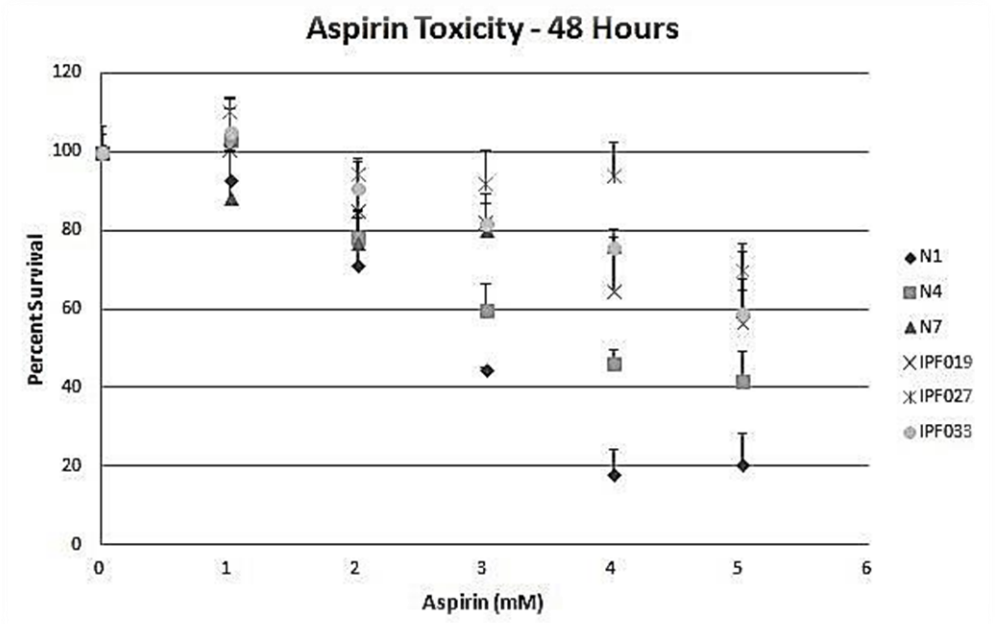

Figure 2A. Percent cell survival of Normal-F (n=3) and IPF-F (n=3) following aspirin exposure (0mM-5mM) for 48 hours.

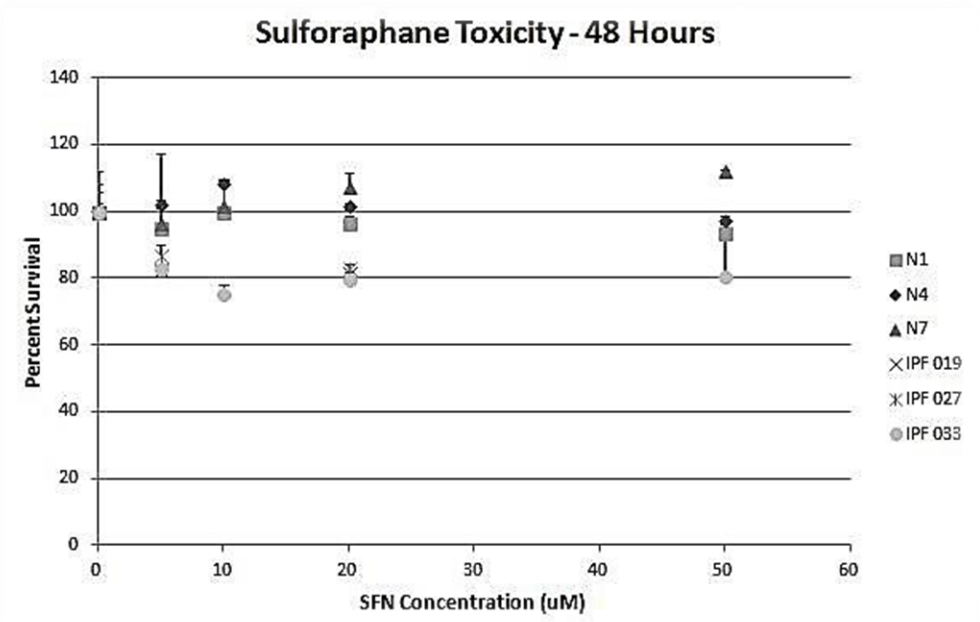

Figure 2B. Percent cell survival of Normal-F (n=3) and IPF-F (n=3) following sulforaphane exposure (0µM-50µM) for 48 hours.

However, when CUR was in combination with ASA and SFN (CAS) using these same sublethal concentrations, cell viability was significantly reduced in normal and IPF fibroblasts (Fig 3) compared to cells treated independently with 20µM CUR. A notable synergistic effect was observed where 87.74±14.25% of the IPF-F cells survived when exposed to CUR alone compared to 50.36±15.04% cell survival after treatment with CAS (P=0.035). Similar results were observed in Normal -F, with a 88.85±20.68% cell survival rate after CUR alone treatment and 23.01±25.79% survival in the presence of CAS (P=0.0160). The preservation of the epithelial cells is maintained to some degree, with an insignificant 33.21±8.24% (P=0.091) decrease in cell survival after 48 hours of CAS treatment.

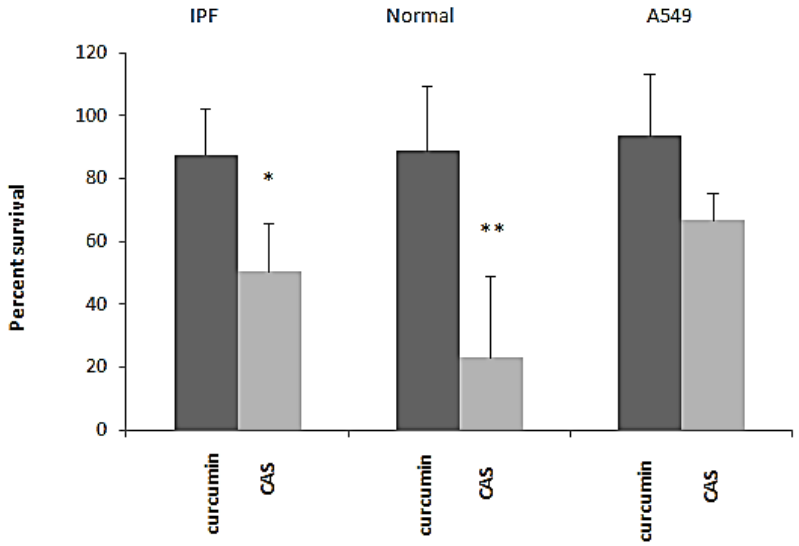

Figure 3. CAS (20µM, 3mM and 40µM, respectively) combination therapy results in significant loss of cell viability in both IPF-F and Normal-F over 48h compared to curcumin (20µM) exposure alone. A549 cell exposure to CAS however did not result in a significant reduction in cell viability. *P≤ 0.05, **P≤ 0.01; represents statistical significance between control and treatment groups as determined by paired t test.

To determine if dual combinations of the agents were capable of the same effect on cell viability, each permutation and dual combination of these agents was carried out. CUR (20μM) paired with ASA (3mM) or SFN (40μM), and ASA and SFN were administered at the same concentrations as in the CAS treatment for 48 hours. In each instance the fibroblast populations were not as sensitive to the dual combinations and exhibited a minimal reduction in cell survival. Thus demonstrating that is the synergism between CUR, ASA, and SFN when applied in combination that results in cell death.

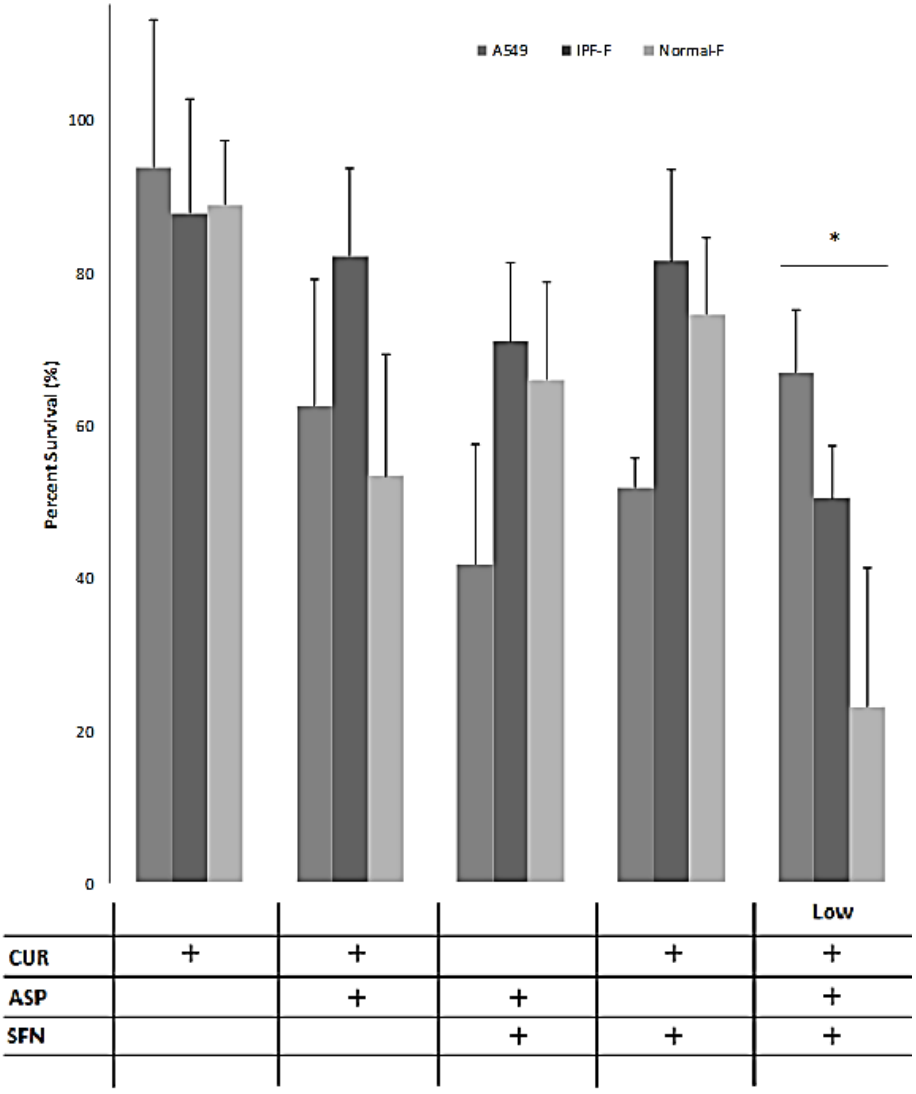

Figure 4. The cell viability of dual drug combination treatments compared to curcumin alone and CAS challenge for 48 hours. *P≤ 0.05; represents statistical significance between control and treatment groups as determined by paired t test.

3.3 CAS induces apoptosis in fibroblasts

The mechanism of cell death induced by CAS was evaluated by terminal deoxynucleotidyl transferase dUTP nick end labelling (TUNEL) assay. The apoptotic index was calculated by counting the number of cells stained red, positive for apoptosis. Exposure to CAS resulted in a 61.1±7% and 45±9% cell survival in IPF-F and N-F respectively, compared to a 73.6±5% cell survival in IPF-F and 66±4% cell survival in N-F after CUR treatment.

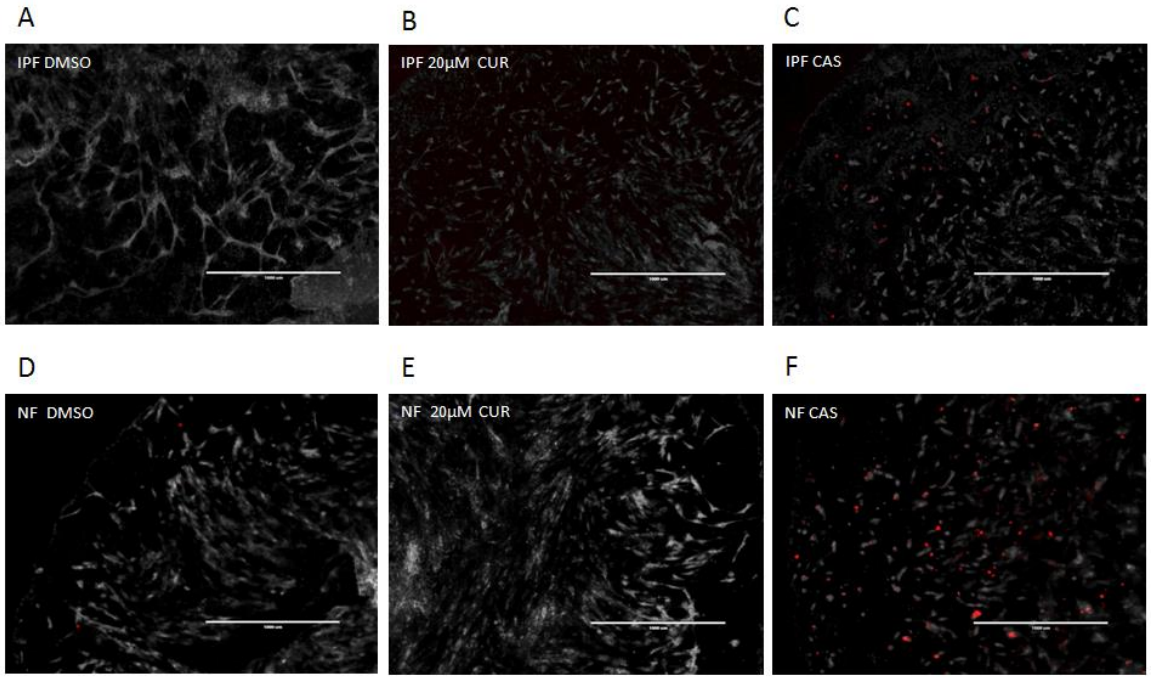

Figure 5. Apoptotic index of CAS (20μM, 3mM and 40μM, respectively) 48h exposure compared to CUR (20μM) and DMSO vehicle control, determined by terminal deoxynucleotidyl transferase dUTP nick end labelling (TUNEL) assay. Red cells are indicative of apoptosis.

CAS-induced apoptotic cell death is Caspase 3/7 dependent. Upon addition of CAS to IPF-F and N-F over a 48 hour time period, there was a significant increase in caspase 3/7 activation (P=0.037 IPF-F, P=0.004 N-F). A nonsignificant increase in level of active caspase 3/7 was observed in the A549 cells, concurrent with the cell survival data (Fig. 3) which shows the preservation of the epithelial cells with CAS treatment.

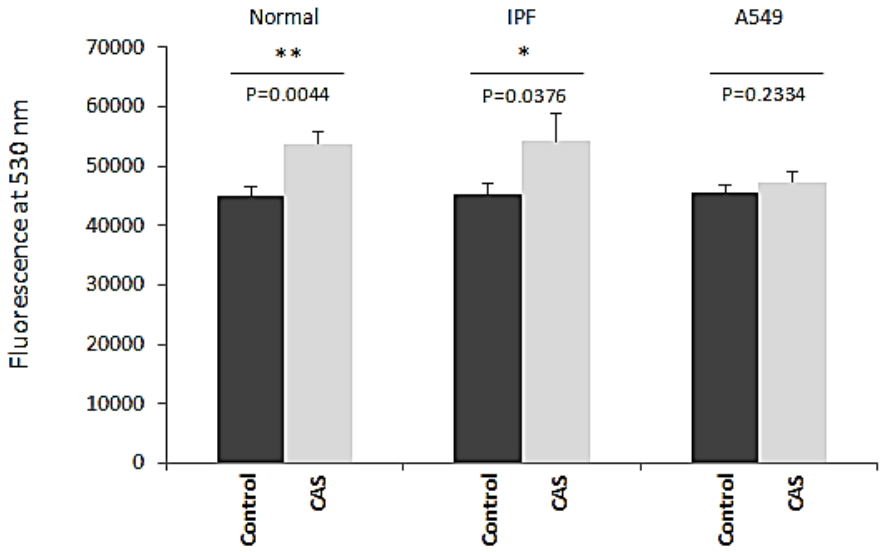

Figure 6. Caspase-3/7 activity of Normal-F, IPF-F, and A549 after CAS challenge for 48 hours compared to vehicle control. *P≤ 0.05, **P≤ 0.001; represents statistical significance between control and treatment groups as determined by paired t test.

Further clarification of the role of apoptosis and caspases 3/7 was accomplished by analysis of the proteolytic cleavage of Poly (ADP-ribose) polymerase (PARP) in IPF-F, Normal-F and A549 cells (Fig 7). CAS exposure resulted in an increase in cleaved PARP compared to vehicle control both IPF-F (+1.32 fold, P=0.072) and N-F (+1.90 fold, P=0.091). Overall, the activation of caspases and the concurrent upregulation of PARP cleavage confirm CAS exposure is an effective synergistic combination of drugs to induce apoptosis in fibroblasts.

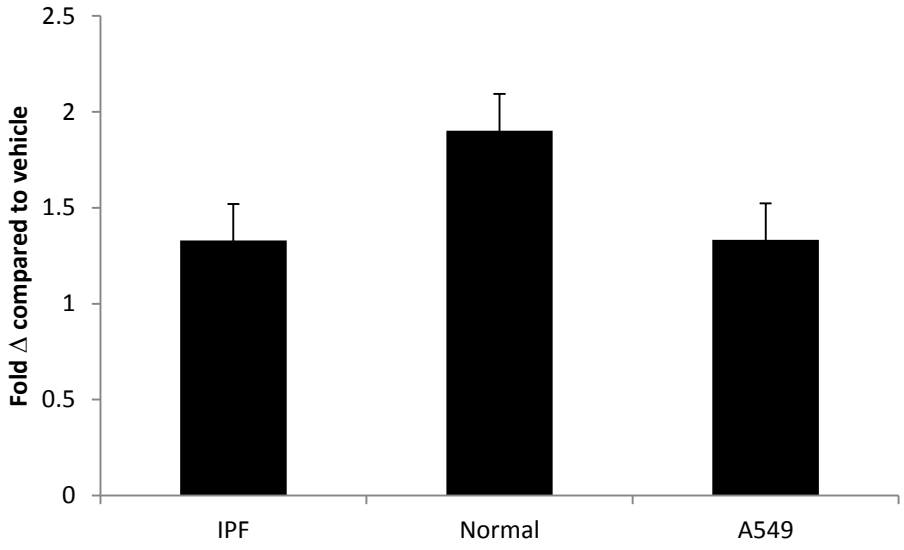

Figure 7. Fold change of cleaved PARP in IPF-F, N-F, and A549 cells following CAS exposure for 48 hours relative to control counterparts with no CAS exposure (vehicle control) as determined by western blot analysis. Data was significant within cell lines; however, this value became non-significant due to standard deviations resulting from the use of primary cell lines.

3.4 CAS activates ERK 1/2 pathway in fibroblasts

To determine the role of the ERK/MEK pathway in CAS induced apoptosis, protein lysates from IPF-F, N-F and A549 were analyzed by western blotting. After 48 hours of CAS exposure, each cell line had increased phosphorylation of p42/44 protein (ERK-1/2) compared to control DMSO. However in IPF-F the expression of phosphorylated p42/44 increases dramatically after 8 hours of CAS treatment. In contrast to the sustained activation of phosphor-p42/44 in N-F, the expression of phospho-p42/44 is transient in IPF-F and the level of p-42/44 phosphorylation begins to decrease after hour 12 of CAS exposure. The different duration of ERK activation may be associated with N-F susceptibility to CAS and noticeable apoptotic resistance in IPF-F compared to N-F after CAS challenge.

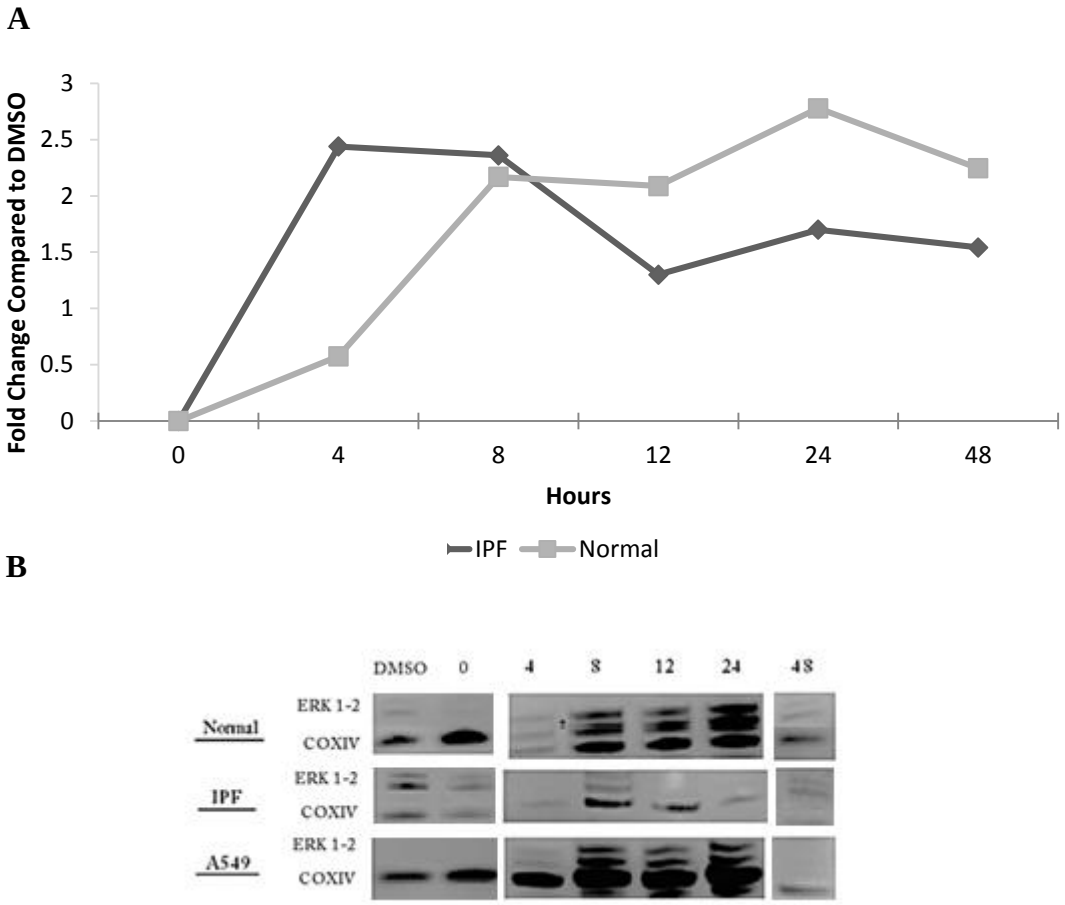

Figure 8. (A) Line graph of densitometry readings for relative phosphorylated ERK-1/2 (44/42 kDa) protein expression in IPF-F vs N-F cells following CAS exposure at various time intervals (0-48 hours). DMSO exposure served as negative vehicle control for all cell lines. Samples were normalized to COX-IV protein expression. **(B)** Western blot analysis of phosphorylated ERK-1/2 (44/42 kDa) protein expression in IPF-F, N-F, and A549 cells following CAS exposure at various time intervals (0-48 hours). COX-IV was used as loading control.

To further investigate the role of ERK activation in CAS induced apoptosis, an MEK1/2 inhibitor, U0126, was used to block MEK1/2 phosphorylation and subsequent ERK1/2 phosphorylation. U0126 pretreatment of the cells did was not able to effectively block the phosphorylation of p42/44, thereby suggesting data CAS induced p-42/44 phosphorylation is MEK independent or through another route. Pretreatment of cells

using U0126 MEK inhibitor partially attenuated CAS-induced apoptosis in N-F (+10%, P=0.551). Since ERK1/2 activation begins to decrease after hour 12 in IPF-F without U0126 pretreatment in a 48 hour CAS challenge, an ERK-inhibitor rescue of cell viability is therefore not observed in IPF-F with U0126 pretreatment. The difference between N-F and IPF-F cell survival after U0126 pretreatment with CAS exposure was insignificant (P=0.075).

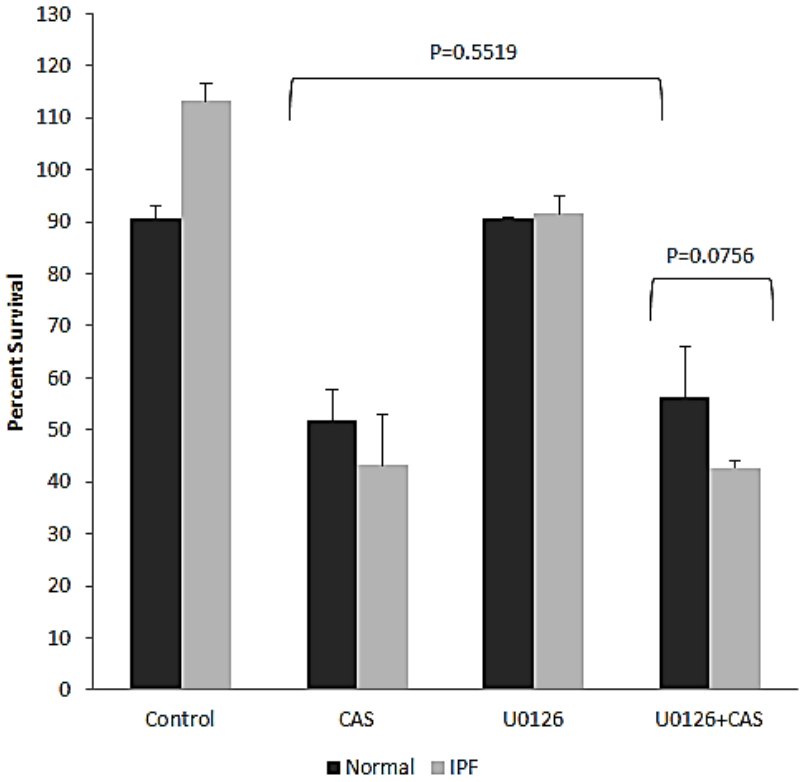

Figure 9A. Combined effect of U0126 and CAS on IPF-F vs N-F cell viability. Cells were pretreated with U0126 (10µM) for 45 minutes before CAS (20µM, 3mM and 40µM, respectively) treatment.

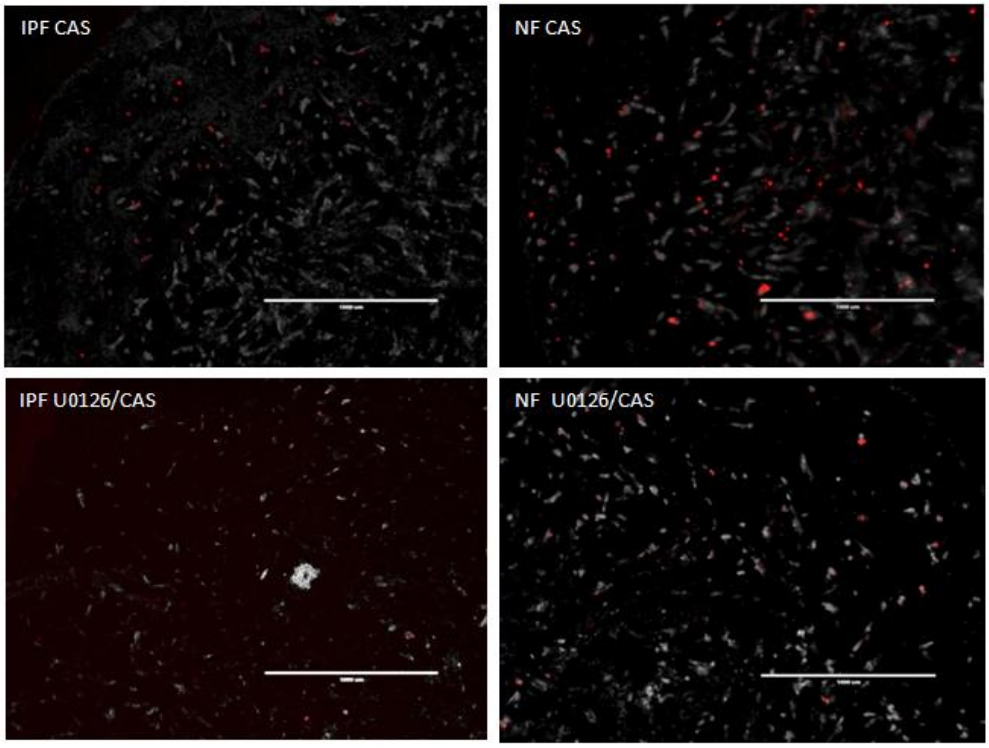

Figure 9B. Terminal deoxynucleotidyl transferase dUTP nick end labelling (TUNEL) analysis of IPF-F and N-F after U0126 (10μM) pretreatment for 45 minutes before CAS treatment, compared to CAS exposure without U0126 pretreatment.

3.5 CAS modulates NFκβ pathway activity in fibroblasts

To determine the role of the NFκβ pathway in CAS induced apoptosis, protein lysates from IPF-F, N-F and A549 were analyzed by western blotting. After 48 hours of CAS exposure, N-F and A549 had decreased phosphorylation of IKK, IKβa, and p-65 protein compared to DMOS vehicle control. Alternatively, IPF-F observed NFκβ activation after 48 hours of CAS challenge.

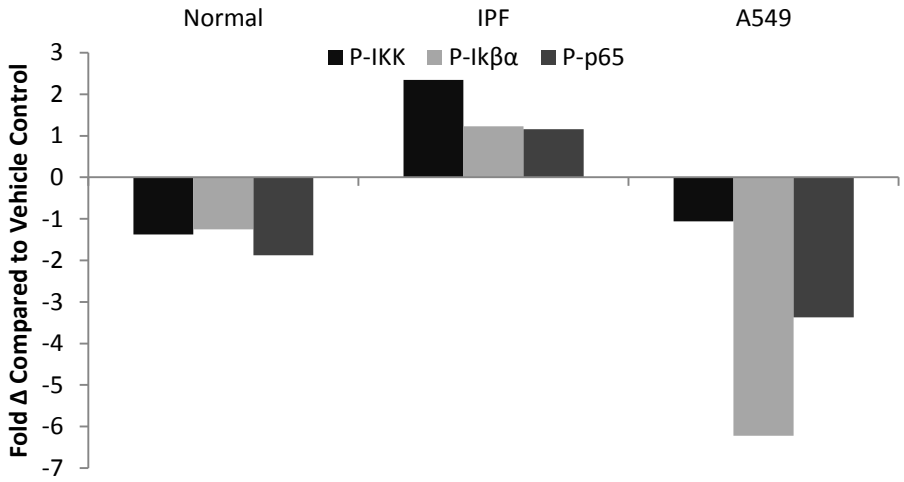

Figure 10. Bar graph of densitometry readings for active phosphorylated IKK, IKβα, and p-65 in IPF-F vs N-F cells following CAS exposure for 48 hours relative to control counterparts with no CAS exposure (vehicle control) as determined by western blot analysis. Samples were normalized to GAPDH protein expression.

Exposure to CAS in N-F resulted in a 1.5 (P=0.0722) fold reduction of phosphorylated AKT and a 2.7 (P=0.00371*) fold increase in BclXL phosphorylation

(Fig 11). Phosphorylated beta-catenin levels were unchanged and displayed no translocation of beta-catenin. Conversely IPF-F cells demonstrated a 1.5 fold (P=0.0386*) increase in AKT phosphorylation, 1.3 fold (P=0.2726) increase BclXL phosphorylation, and 7.37 (P=0.00627*) fold decrease in phosphorylated beta-catenin (Fig. 11) and nuclear translocation of the protein was confirmed by IHC and absence of phosphorylated β-catenin in isolated cytosolic protein fractions (Fig. 12).

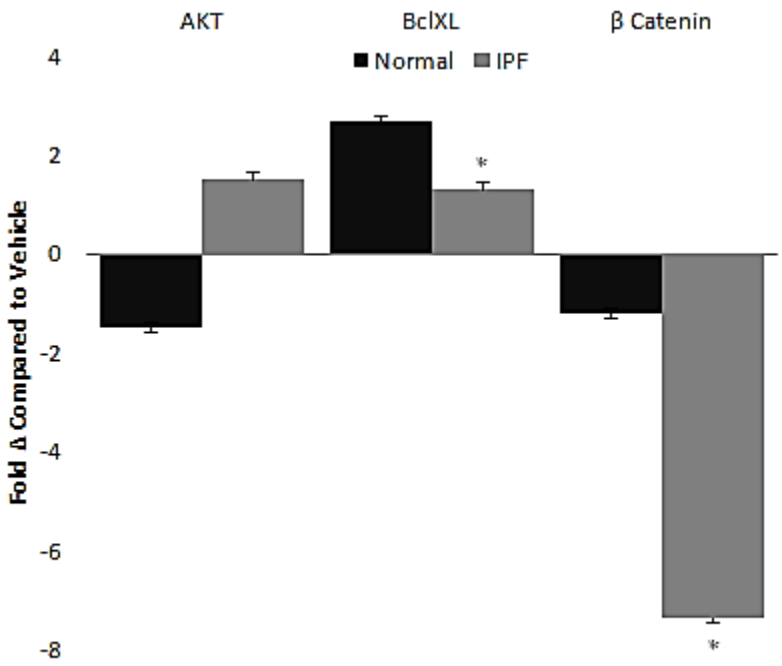

Figure 11. Bar graph of densitometry readings for active phosphorylated AKT, phosphorylated BclXL, and phosphorylated cytosolic β-Catenin in IPF-F vs N-F cells following CAS exposure for 48 hours relative to control counterparts with no CAS exposure (vehicle control) as determined by western blot analysis. Samples were normalized to GAPDH protein expression *P≤ 0.05; represents statistical significance between control and treatment groups as determined by paired t test.

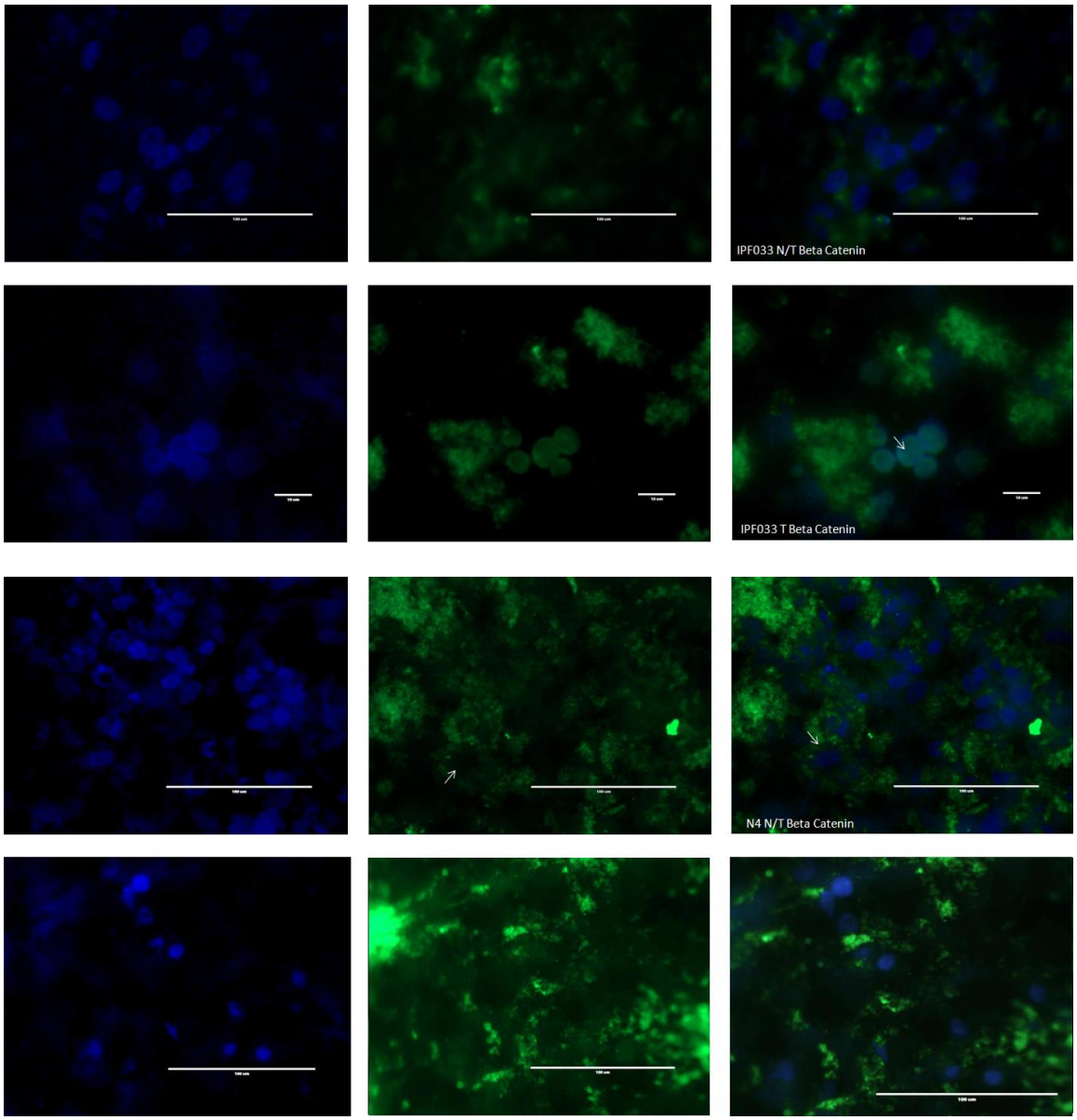

Figure 12. ICC analysis of IPF-F and N-F, CAS and DMSO vehicle control, for β-catenin translocation at 100x objective magnification. Left: Blue DAPI staining of corresponding nucleus. Middle: Green fluorescent staining is representative of β-catenin localization. Right: Overlay of both β-catenin (green) and nuclei (blue) images. Teal is representative of β-catenin translocation into the nucleus.

3.6 CAS inhibits the activation status of fibroblasts

Exposure of IPF fibroblasts to CAS resulted in significant changes in expression of markers of fibroblast activation at the gene level. Specifically, alpha-SMA (ACTA2) gene expression in IPF-F decreased by -1.28 fold after CAS treatment compared to untreated IPF-F. Normal fibroblasts and A549s did significantly change their alpha-SMA gene expression. CAS exposure also resulted in a significant inhibition of collagen A1 (COLA1) gene expression in all cell tested, specifically a -25.19 fold change in gene expression for IPF-F, while a -15.34 and -5.18 fold change was observed in N-F and A539 respectively. CAS exposure also resulted in a significant reduction in Cyclin D1gene expression in both fibroblast cell lines, IPF-F (-8.89) and N-F (-5.73), however A549 seemed unaffected, which is potentially concurrent with survival data showing the preservation of the epithelial alveolar lung cells during CAS challenge.

The apoptotic resistance observed in the IPF-F compared to N-F is highlighted again by the differential expression of Nrf2, a gene potentially induced by curcumin which facilitates an antioxidant response and promotes a protective effect. Nrf2 is downregulated in N-F by -1.39 fold after CAS treatment. Conversely, Nrf2 expression is increased by 1.49 fold compared to untreated in IPF-F. The difference between IPF-F and N-F expression of Nrf2 is approximately 3 fold differences.

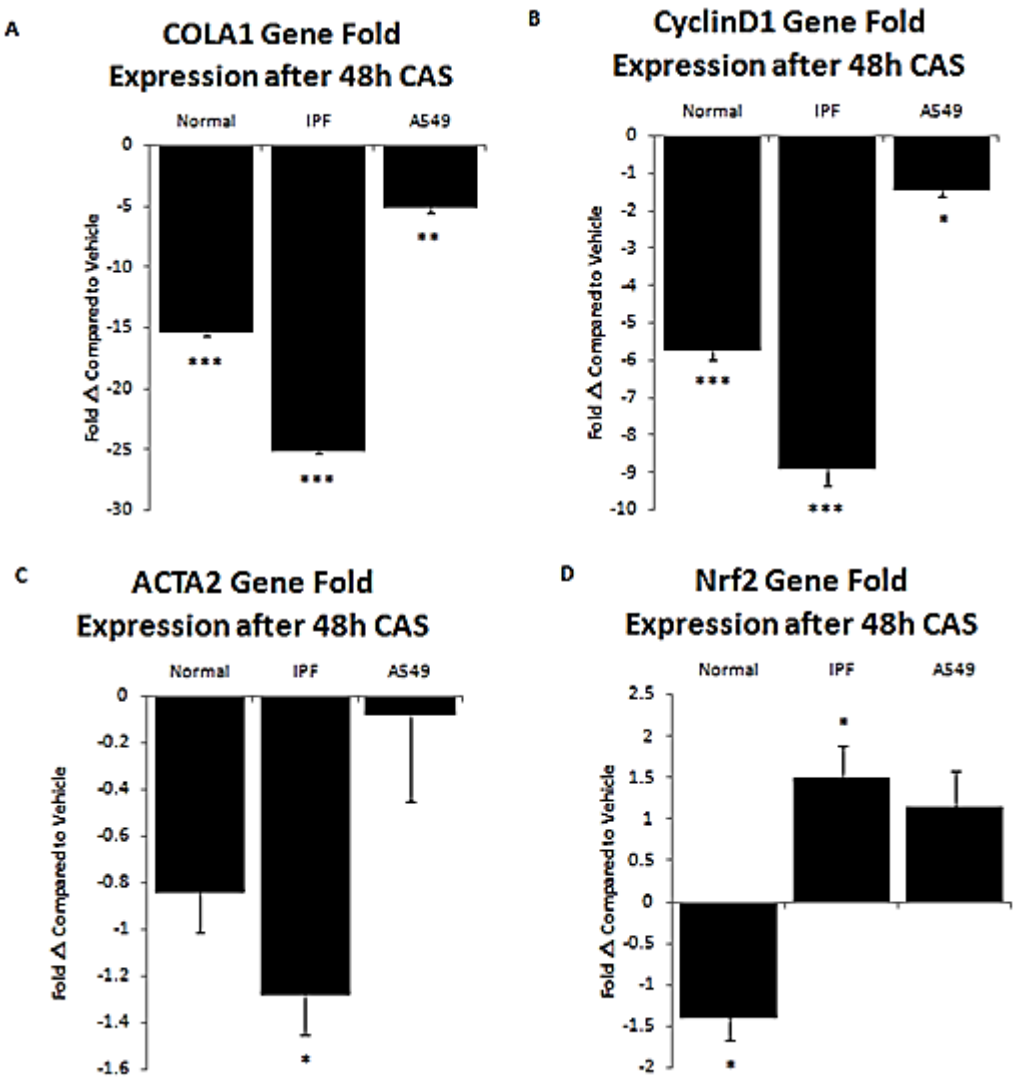

Figure 13. Fold change in mRNA of fibroblast markers (Cyclin D, COLA1, ACTA2) and Nrf2 following CAS challenge in Normal-F, IPF-F, and A549 for 48 hours. Fold change is compared to DMSO vehicle control. *P≤ 0.05, **P≤ 0.01, ***P≤ 0.001; as determined by t test.

3.7 CAS summary

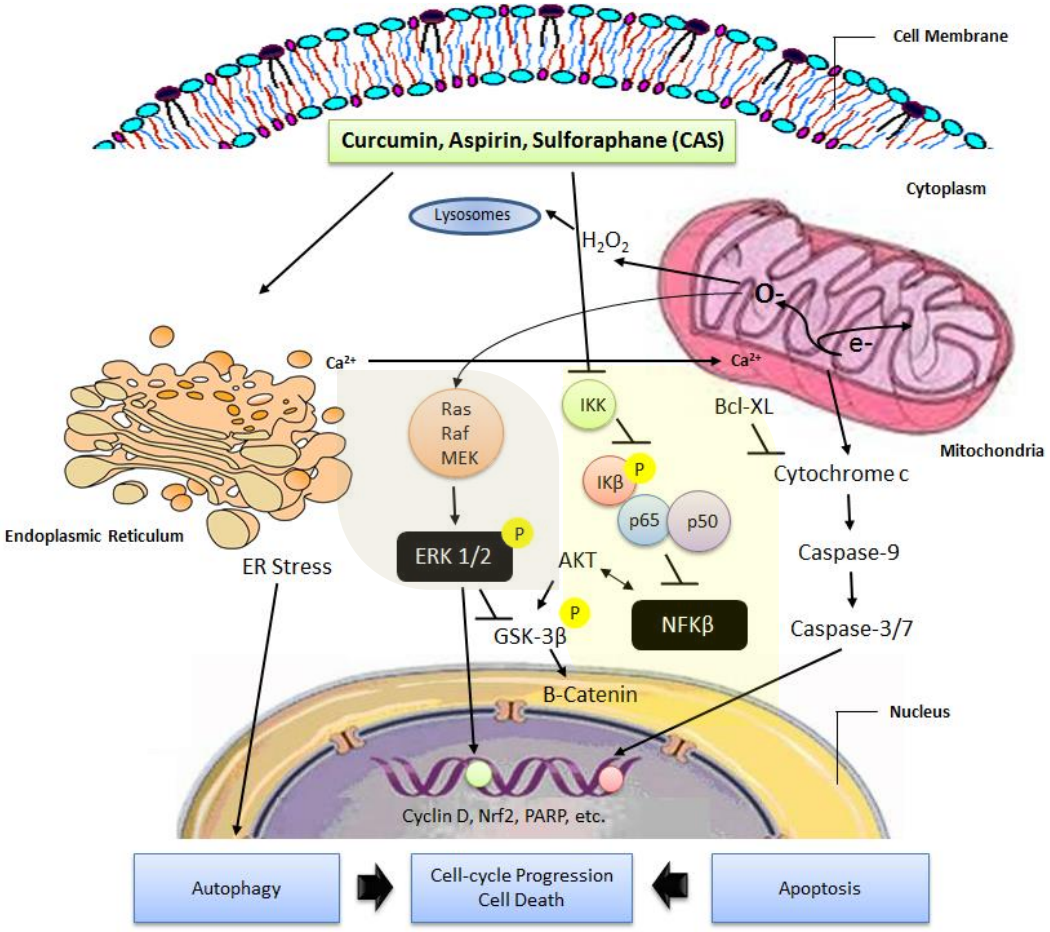

Figure 14. The proposed mechanism of CAS in the reduction of cell viability and the inhibition of fibroblast activation. CAS induction of endoplasmic reticulum stress leads to calcium release from the ER. The uptake of this calcium by the mitochondria causes destabilization of the mitochondrial membrane and disruption of the electron transport chain causing substantial ROS production. Once the membrane is permeable to cytochrome c, the release of cytochrome c into the cytosol activates capase-3/7 pathway. Active caspase-3/7 and consequential proteolytic cleavage of PARP commits the cell to an apoptotic fate. Furthermore, ER stress pathway may induce autophagy in an attempt to eliminate the dysfunctional mitochondria. Low dose curcumin in CAS triggers the chemoprotective mechanism of autophagic cell death. Normal-F ERK-1/2 pathway sustained activation is different from the transient activation of ERK-1/2 observed in IPF-F (highlighted green). Normal-F NFKβ pathway inhibition is different from the activation of NFKβ observed in IPF-F (highlighted yellow).

4. DISCUSSION

Curcumin is a hydrophobic polyphenol, shown to have a broad range of antioxidant, antibacterial, antifungal, antiviral, anti-inflammatory, anti-proliferative, and pro-apoptotic properties (Aggarwal, 2009). Curcumin has also been reported to have anti-fibrotic capabilities in studies on wound healing, liver fibrosis and in lung fibrosis models (Lin, 2009; Zhang, 2011; Smith, 2010; Chen, 2008). At the molecular level, curcumin has been reported to play an anti-fibrogenic role by modulating transcription factors such as transforming growth factor beta (TGF-β) (Chen, 2013), platelet derived growth factor (PDGF), fibroblast growth factor (FGF) and tumor necrosis factor alpha (TNF-α) (Shishodia, 2013; Hua, 2013; Das, 2014), all of which are implicated in the pathogenesis of IPF.

Initially we investigated the anti-fibrotic capabilities of curcumin over a range of concentrations and exposure times using a novel in vitro fibroblast model system and lung alveolar epithelial (A549) cell line model. We found that exposure to curcumin resulted in a significant dose and time dependent reduction in the viability of IPF-F, normal-F and A549 cells. These data are in agreement with previous studies where curcumin exposure has resulted in reduction of cell survival and induction of apoptosis (Aggarwal, 2009; Gupta, 2013; Bush, 2001). However, what is notable and novel is that curcumin preferentially decreased viability and induced apoptosis in lung fibroblasts, with relative preservation of epithelial cells. This selective targeting makes curcumin an attractive potential agent for use in IPF, where fibroblast overpopulation and alveolar cell

death are major concerns. The selective kill capability of curcumin has been previously reported in other cell types, most notably with tumor cells. Although a promising drug candidate for IPF, the poor bioavailability of curcumin is a limiting factor. Therefore the overall aim of the study was to investigate the synergistic potential of aspirin and sulforaphane to potentiate curcumin's effect on the viability, proliferation and activation status of primary pulmonary IPF (IPF-F) and normal (N-F) fibroblasts. Based on the hyper-proliferative anti-apoptotic phenotype observed within the IPF-F population, we hypothesized the induction of apoptosis *in vitro* using a combination of curcumin, aspirin, and sulforaphane (CAS) would reveal differences in apoptotic mechanisms between IPF fibroblasts and normal fibroblasts. A number of mechanisms have been suggested for this selectivity such as increased cellular uptake of curcumin, lower glutathione levels and constitutively active NF-kappa-beta in these cells (Shishodia, 2005; Syng-Ai, 2004). We explored differences in CAS-mediated NFKβ survival pathway and ERK1/2 pathway. We also focused on the effect of CAS on the activation status and proliferative state of fibroblasts based on CAS's ability to regulate alpha-SMA, COLA1, and cyclin D expression.

4.1 CAS-induced apoptosis

The cell proliferation and viability assays demonstrated that low concentrations of curcumin, aspirin, and sulforaphane when used in combination has a synergistic apoptotic effect in IPF-F and N-F (Fig. 3-4). The anti-proliferative and pro-apoptotic effects of curcumin are mediated by abrogating genes such as Bcl-2, cyclin D1, IL-6, COX-2, and MMP-9 (Aggarwal, 2004). Curcumin has been combined with drugs like Vinorelbine,

Celecoxib, Beta-phenylethyl isothiocyanate (PEITC), oxaliplatin, 5-Fluorouracil, gemcitabine, and paclitaxel to increase their cytotoxic effect. Human squamous cell lung carcinoma cells treated with Vinorelbine and curcumin observed a significant reduction in cell survival compared to Vinorelbine treatment alone (Sen, 2005). Celecoxib was used in combination with curcumin to arrest cell growth and induce apoptosis in osteoarthritis synovial adherent cells (Lev-Ari, 2006), colorectal cancer cells (Lev-Ari, 2005) and pancreatic adenocarcinoma cells (Lev-Ari, 2005). Since Celecoxib is contraindicated for long-term use in treatments due to its cardiovascular toxicity, it is a novel potential treatment option to utilize curcumin's synergistic effects in order to lower concentrations of Celecoxib. This strategy can be applied to other disease treatments where agents can be dosed at lower and safer concentrations. Many chemotherapeutic drugs have been studied in combination with curcumin in the last years because a multi-target based drug approach decreases the probability that cancer cells will develop resistance to chemotherapeutic agents.

The treatment of complex human diseases, such as IPF, is not likely to involve a single-target and therefore single-drug approaches may not be as potent when compared to a multi-target based approach that work in synergy by different mechanisms of action. We demonstrate the efficacy of using low dosages of aspirin and sulforaphane in combination with curcumin to eliminate primary human-derived fibroblasts, while preserving the alveolar lung epithelial cells to some degree (Fig. 4).

Mitochondrial associated apoptosis

Curcumin treatment has been shown to upregulate ER stress markers CHOP and Bip/GRP78 (Lee, 2015). ER stress causes calcium release and subsequent uptake of this calcium by the mitochondria. Calcium ion influx effects mitochondrial electron transport chain (ETC) functionality, causing a significant production of superoxide anions and hydrogen peroxide within the cell. These reactive oxygen species (ROS) leads to the formation of pores in the mitochondrial membrane through which cytochrome c is released. The activation of this classical apoptotic pathway by CAS was confirmed by evidence of caspase 3/7 activation and proteolytic PARP cleavage through ApoGLO and western blotting, respectively. As shown in Figure 6, there were marked increases in the levels of cleaved caspase3/7 in CAS treatment compared with curcumin alone. Of note, were the increases of downstream proteolytic cleavage of PARP after exposure to CAS in IPF-F and N-F (Fig. 7). Although the IPF-F displayed less PARP cleavage than N-F, due the heterogeneity in primary cell lines, this difference was not significant. The levels of PARP cleavage and caspase activation in IPF-F and N-F are comparable to their respective cell viability data after CAS challenge (Fig. 3; Fig.5). These data are in agreement with previous observations in PaCa-2 and Panc-1 cells treated with CAS (Thakkar, 2013). Thakkar et al. concluded in their study that CAS was extremely effective in inducing apoptosis of pancreatic cancer cells. Similarly, CAS-induced apoptosis reduced fibroblast cell viability in our study.

Interestingly, microarray analysis of IPF fibroblasts compared to normal fibroblast revealed sacro/endoplasmic reticulum calcium ATPase 2 (SERCA2) is

upregulated 1.78 fold. The major Ca^{2+} pump, SERCA, is dysregulated in cancer cells and contributes to their proliferative, apoptotic-resistant phenotype. Data from ovarian cancer cells showed that SERCA expression is higher in cancer than in normal tissues, similar to our findings when comparing IPF fibroblasts to normal fibroblasts. Many studies in various types of cell lines including ovarian cancer cells, colorectal cancer cells, and lung cancer cells have shown that the addition of a Ca^{2+} chelator protects curcumin-induced apoptosis, thereby suggesting that curcumin apoptosis relies on disrupting cytosolic Ca^{2+} homeostasis. A recent study using curcumin-treated ovarian cancer cells further demonstrated significant elevation of cytosolic calcium concentration through the inhibition of SERCA (Seo, 2016). However, further investigations are required to make reports on the role of increased cytosolic Ca^{2+} and ER stress in CAS-induced apoptosis.

Autophagy

In a recent article published in *Cell Death Discovery*, it was reported that curcumin at very low doses (≤1μM) serves protective functions as an antioxidant. At moderate concentrations of 10-15μM, curcumin induces autophagy. While at concentrations above 25μM, curcumin operates as an apoptotic inducer (Moustapha, 2015). The concentration of curcumin we used in the combinatorial treatment (CAS) is in between the moderate dose and the high dose (20μM). If curcumin has both antioxidant and pro-oxidant properties that are linked to autophagic and apoptosis activation processes, then it is possible that differential expression of SERCA activity can induce a chemoprotective mechanism of cell death in IPF-F (autosis), and MOMP apoptosis in N-F when exposed to CAS. Additional studies involving the staining of autophagic

vacuoles, and western blotting of autophagosome markers, LC3-I and LC3-II, would be needed to make further conclusions.

CAS-induced apoptosis is p-53 independent

In the extrinsic apoptotic pathway, proapoptotic ligands such as CD95L/FasL in human melanoma cells are activated when treated with curcumin (Bush, 2001). Depending on the cell type, the extrinsic pathway can either be p53 dependent or p53 independent (Jee, 1998). Many tumors have a p53 mutation, causing antineoplastic agents to be less efficacious. In a recent study investigating p53 gene mutations in pulmonary fibrosis patients, out of 10 tissue samples that demonstrated overexpression of p53 protein by immunostaining: nine (90%) exhibited point mutations and eight (80%) exhibited heterogeneous point mutations of the p53 gene (Hojo, 1998). Since curcumin is able to induce cell death through a pathway which circumvents p53 translocation into the nucleus (Bush, 2001), it may be a potential therapeutic for cells with a p53 mutation. CAS challenge induced apoptosis independent of p-53 in N-F or IPF-F (Supplemental Data). However, the data warrants additional studies to determine if this mode of action is driven by curcumin.

4.2 ERK-1/2 pathway in CAS-induced apoptosis

CAS induces ERK-1/2 activation in fibroblasts

Thakkar et al. demonstrated CAS induces ERK activation in pancreatic cancer cells (Thakkar, 2012). We observed through western blot analysis that incubation of IPF-F and N-F with CAS produced increased phosphorylation of p42/44 subunits of ERK-1/2 compared to DMSO controls after 48 hours. Next, we investigated the activation of ERK-

1/2 at different time intervals for 4, 8, 12 and 24 hours. The expression of phosphorylated ERK-1/2 was markedly increased after 8 hours in N-F and activation levels are sustained (Fig. 8A-B). Contrastingly, IPF-F showed transient ERK-1/2 phosphorylation which begins to decrease in phospho-p42/44 protein expression after 12 hours of CAS exposure. Persistent ERK activation is MEK1/2 dependent in CAS-induced apoptosis of pancreatic cancer cells (Thakkar, 2012).

Role of ERK1/2 in fibroblast cell viability

In order to verify the involvement of ERK-1/2 activation in CAS-induced apoptosis of fibroblasts, we used a MEK1/2 inhibitor, U0126. The cell viability assay comparing U0126+CAS treated cells and cell treated with CAS alone, yielded minimal rescue of cell survival (Fig. 9). Western data showed that even after U0126 pre-treatment, the cells still express phosphorylated ERK-1/2. However, when comparing the cell survival between IPF-F and N-F after U0126+CAS treatment, that difference had a p-value bordering significance of 0.07. Using a greater sample size may have yielded a statistically significant result. The data suggests that CAS differential activation of ERK-1/2 may be MEK1/2 independent. Although we could not mitigate CAS-induced apoptosis through inhibition of MEK1/2 pathway, it does not equivocally eliminate its role in the drug mechanism. MEK1/2 is capable of autophosphorylation, and thereby still activating downstream effector kinases such as ERK-1/2. Ras is not the only MAP3K activator upstream of Raf for regulating ERK-1/2. Protein kinase C (PKC) alpha has been shown to activate Raf-1 (Kolch, 2005). Mos, TPL2 protooncogene, MLK-like mitogen-activated protein triple kinase (MLTK), interleukin-1 receptor-associated kinase (IRAK)

have also been shown to activate ERK-1/2 (Gotch, 1995; Salmeron, 1996; Gotch, 2001; MacGillivray, 2000). The activation of ERK-1/2 induced by different initiating signals results in the phosphorylation of different substrates. Over 150 substrates have been identified and have an effect on cell cycle, scaffold and cytoskeletal arrangement, and other types of proteins (Yoon, 2006). Therefore, differential ERK-1/2 phosphorylation at different amino acids induced by the MEK1/2 inhibitor may result in an altered outcome of cell survival, as observed in our population of IPF-F. However, further studies involving mass spectrometry of ERK-1/2 proteins would shed light on its potentially different phosphorylation sites in IPF-F and N-F after CAS challenge.

4.3 NFKβ pathway in CAS-induced apoptosis

CAS modulates the NFKβ pathway

The nuclear NFKβ complex containing p65 (Rel A) and p50 (NFKβ1) is a multifunctional transcription factor associated with regulating cell cycle, cell differentiation, and inflammation processes. The inactive NFKβ-IKβ complex remains cytosolic until the inhibitory molecule, IKβ, is phosphorylated and tagged for proteasomal degradation. This allows for the translocation of NFKβ, subsequent accumulation of the transcription factor, and modulation of NFKβ-dependent gene expression. Genes such as cyclin D, survivin, VEGF, Bcl-2, and COX-2 are induced by NFKβ. As shown in Fig.13B, cyclin D is downregulated in N-F, IPF-F, and A549 after 48 hours of CAS exposure.

All three proteins in the NFKβ pathway: IKK, IKβ, and p65 were also downregulated after CAS challenge in all the cell lines with the exception of IPF-F (Fig.

10). The suppression by curcumin of the transcription factor NFκβ reported in melanoma cells, CD138+ cells, and pancreatic cancer cells, inhibits cell survival and cell proliferation genes (Bharti, 2004; Marin, 2007; Li, 2004). Curcumin has been implicated in the up-regulation of pro-apoptotic proteins of the Bcl-2 family in cancer cells (Woo, 2003; Mukhopadhyay, 2001). Bcl-xL and Bcl2 are downstream anti-apoptotic factors of NFKß survival pathways. In gastric and colon cancer cells, curcumin-induced cell death was initiated by Fas signaling pathway and Caspase-3 activation leading to the cleavage of PARP and the inhibition of Bcl-xL (Moragoda, 2001). An excess of pro-apoptotic proteins and lack of anti-apoptotic signals will converge in the mitochondria and cause a disruption in the membrane potential, inducing apoptosis.

Differential NFKβ inhibition may contribute to IPF-F apoptotic resistance profile

Nuclear factor kappa beta promotes cell survival by regulating genes such as survivin, Bcl-XL, XIAP, and Myc. After 48 hours CAS exposure, NFKβ down-regulation was not observed in IPF-F, in contrast to N-F and A549 (Fig. 10). As a result, downstream expression of survival proteins such as Bcl-XL was not inhibited (Fig. 11). Bcl-XL is a transmembrane molecule in the mitochondria. It is a member of the Bcl-2 family of proteins, and acts as a pro-survival protein by preventing the release of mitochondrial contents such as cytochrome c, which would lead to caspase activation. Caspase3/7-mediated PARP cleavage is comparatively at lower levels in IPF-F than N-F (Fig. 7). Concurrent with these observations are the results from both the TUNEL and cell viability assays, which demonstrates the slight increase in percentage of IPF-F cell

survival. This data is supports a hypothesis of pro-survival NFKβ playing a role in IPF-F apoptotic resistance during CAS challenge.

Microarray analysis comparing IPF-F to N-F showed a 1.92 fold upregulation in NFKβ p50 subunit. The overexpression of NFκβ induced by Rhotekin (Liu, 2004) or inherently upregulated in disease states of human mantle cell lymphoma (Shishodia, 2005), confers an apoptotic resistant profile in the cell types. NFκβ and Iκβ kinase are constitutively active in human pancreatic cancer cells (Li, 2004). These cells with constitutively active NFKβ display a hyperproliferative antiapoptotic phenotype. The differential activation of NFKβ in IPF-F and N-F after CAS challenge could be attributed to the constitutively higher levels of NFKβ activity in IPF-F. With a greater sample size in the microarray analysis, the fold change of NFKβ proteins may reach a level of statistical significance.

Additional potential regulators of NFKβ

Recent studies by Jutooru et al. have demonstrated the effects of curcumin are (Sp) Specificity Protein-dependent. In their study, they observed the inhibition of Panc28 and L3.6pL cell growth through curcumin-induced decrease of p50 and p65 proteins and decrease of Sp1, Sp3, Sp4 transcription factors that are overexpressed in pancreatic cancer cells (Jutooru, 2010). Because both Sp transcription factors and NFKβ regulate cyclin D, survivin, and VEGF, it was hypothesized that there was crosstalk between the two pathways. Direct evidence for the role of Sp transcription factors in regulating NFKβ was obtained by RNA interference. The results demonstrated that both p50 and p65 are Sp-regulated genes and that inhibition of NFKβ by curcumin is dependent on the

downregulation of Sp 1, Sp3, and Sp4 (Jutooru). Additional studies are required to elucidate whether CAS follows a similar mechanism of NFKβ modulation in fibroblasts.

4.4 Beta-Catenin translocation

Chilosi et al. demonstrated an aberrant activation of the Wnt/β-catenin pathway in IPF (Chilosi, 2003), suggesting that this event might play an important role in the irreversible remodeling of the interstitial architecture of the lung. Nuclear translocation and accumulation of beta catenin activates the TCF/LEF family of transcription factors and may induce the expression of several target genes involved in IPF pathogenesis, such as matrix metalloproteinases (MMP2, MMP3, and MMP9), cyclin D1, matrilysin, and fibronectin. To investigate the localization of beta catenin after CAS challenge, ICC of IPF-F challenged with CAS demonstrated beta catenin translocation into the nucleus, while beta catenin remained in the cytosol of N-F (Fig. 12). The mechanism by which beta catenin is regulated in fibroblasts in response to apoptotic challenge is not fully understood; however, a few pathways have been implicated.

Akt crosstalk regulation of β-catenin

IPF fibroblasts constitutively expressed increased basal levels of SPARC, plasminogen activator inhibitor-1 (PAI-1), and active β-catenin compared with control cells (Chang, 2010). Recent studies reported, control of basal PAI-1 expression in IPF fibroblasts was regulated by SPARC-mediated activation of Akt, leading to activation of β-catenin (Chang, 2010). Additionally, Chang et al. observed IPF fibroblasts (but not control fibroblasts) were resistant to plasminogen-induced apoptosis and were sensitized

to plasminogen-mediated apoptosis by inhibition of SPARC or β-catenin. These findings uncover a newly discovered regulatory pathway in IPF fibroblasts that is characterized by elevated SPARC, giving rise to activated β-catenin, which regulates expression of downstream genes, such as PAI-1, and confers an apoptosis-resistant phenotype. Concurrent with this study by Chang et al., SPARC was 2.4 fold upregulated in IPF fibroblast (Emblom-Callahan, 2010). Western blotting also provides evidence of increased Akt activation in IPF-F compared to N-F (Fig. 11). Additionally, our microarray analysis showed PAI-1 is 3.18 fold upregulated in our IPF-F population compared to its normal counterparts. Taken together, IPF-F responded to CAS challenge by activating Wnt/β-catenin signaling to potentially promote survival of fibroblasts in a high stress environment. Further investigations are warranted and should explore the relationship between CAS-mediated apoptosis and Wnt/β-catenin pathway in the context of IPF.

GSK-3/β-catenin pathway via ERK activation

The rapid replacement of epithelial cells with mesenchymal cells in IPF is only partially explained by the increased apoptosis of alveolar epithelial cells. It has been previously described both *in vitro* and *in vivo* that there is significant increase in epithelial cell death. Enhancing this apoptotic resistance is transforming growth factor beta1 which is secreted by surrounding epithelial cells. TGF-beta1 targets the GSK-3/β-catenin pathway via ERK activation in the transition of human lung fibroblasts into myofibroblasts (Caraci, 2008). We observed through western blotting, ERK-1/2 activation (Fig. 8A) and inactivated phosphorylated GSK-3 (Supplemental Data) in IPF-F

after CAS challenge. Caraci et al. proposes this is a potential mechanism for β-catenin translocation in myofibroblasts. Future investigations to demonstrate the role of GSK-3 inactivation in the promotion of β-catenin translocation using a GSK-3 inhibitor may shed light on the differential β-catenin localization in IPF-F after CAS challenge.

5. CONCLUSION

CAS is a low-dose combinatorial regimen, effective in triggering apoptosis in fibroblasts synergistically, while preserving to some degree the lung alveolar epithelial cell population. Although the precise mode of action of CAS is unclear due to the multifactorial nature of a combination therapy, the study has highlighted the contrasting differences between normal fibroblasts and IPF fibroblasts when under environmental stress. Given the contrasting apoptotic mediators in ERK-1/2 and NFKβ pathways, as well as differential expression of potential cross-regulating proteins, suggest there may exist differences in responses to environmental stimuli depending on the fibroblast population. Therefore, isolating the different fibroblast populations directly from human lung tissue allowed for the investigation of the abrogated apoptotic stimuli responses within this novel population of cells uncontaminated by other cell types. The *in vitro* behavior of these cells may more adequately reflect the *in vivo* behavior. The novel population of primary IPF fibroblasts are not induced via an inflammatory route as in the bleomycin model, but sourced centrally from the diseased lung. Through the panning method of isolation, the cells are cultured directly out of the body allowed for the unique opportunity to elucidate inherent differences between normal fibroblasts and IPF-derived human fibroblasts.

This study will further the understanding of the disease and enhance discovery work for future applications towards the selection of IPF fibroblast populations. The development of therapeutics aimed to preserve the epithelial and normal fibroblast

populations is dependent on identifying mediators of cell death and growth specific to IPF fibroblasts.

Future Directions

The influence of apoptosis resistance on the IPF fibroblasts population is a highly controversial topic. While some suggest they are more apoptosis resistant (Thannickal 2006; Fattman 2008), others, on the contrary, suggest IPF fibroblasts exhibit an increased rate of apoptosis derived from lung tissue explants (Ramos 2001). Nonetheless, we have found that a wide array of apoptosis genes are altered in IPF fibroblasts, many of which are pro-apoptotic in nature (Supplemental Data). The increased resistance observed in IPF fibroblasts may be a result of an underlying physiological difference such as an altered mitochondria or endoplasmic reticulum that confers a change from the normal apoptotic route of regulated, healthy fibroblasts. Existing therapies have not exploited a cell target that is selective for IPF fibroblasts. Many questions arise from our findings, which justify further characterization of apoptotic mechanisms in IPF fibroblasts. Determining the differences in cell death between healthy fibroblasts and diseased fibroblasts may be critical to future studies in drug design or in the discovery work of a biomarker. This study has the potential to provide new insights and applications towards the eradication of IPF.

APPENDIX A: SUPPLEMENTAL DATA

Unigene	Gene Name
Hs.31210	B-cell CLL/lymphoma 3
Hs.478588	B-cell CLL/lymphoma 6
Hs.159494	Bruton agammaglobulinemia tyrosine kinase
Hs.164419	DnaJ (Hsp40) homolog, subfamily C, member 5
Hs.411081	FYVE, RhoGEF and PH domain containing 3
Hs.173438	Fas apoptotic inhibitory molecule
Hs.624900	GTP cyclohydrolase 1
Hs.502528	NADH dehydrogenase (ubiquinone) Fe-S protein 3, 30kDa (NADH-coenzyme Q reductase
Hs.655088	SAP30 binding protein
Hs.653163	TAF9 RNA polymerase II, TATA box binding protein (TBP)-associated factor, 32kDa
Hs.9613	antiopoietin-like 4
Hs.1584	cartilage oligomeric matrix protein
Hs.370771	cyclin-dependent kinase inhibitor 1A (p21, Cip1)
Hs.435051	cyclin-dependent kinase inhibitor 2D (p19, inhibits CDK4)
Hs.237886	death-associated protein kinase 2
Hs.5120	dynein, light chain, LC8-type 1
Hs.513153	furin (paired basic amino acid cleaving enzyme)
Hs.1197	heat shock 10kDa protein 1 (chaperonin 10)
Hs.593339	high-mobility group box 1; high-mobility group box 1-like 10
Hs.583348	inhibin, beta A
Hs.76884	inhibitor of DNA binding 3, dominant negative helix-loop-helix protein
Hs.126256	interleukin 1, beta
Hs.522819	interleukin-1 receptor-associated kinase 1
Hs.297413	matrix metallopeptidase 9 (gelatinase B, 92kDa gelatinase, 92kDa type IV Collagenase
Hs.633762	nicotinamide nucleotide adenylyltransferase 1
Hs.493716	phosphatase and tensin homolog; phosphatase and tensin homolog pseudogene 1
Hs.466383	pleckstrin homology domain containing, family F (with FYVE domain) member 1

Hs.631574	pleckstrin homology domain containing, family G (with RhoGef domain) member 2
Hs.602085	pleckstrin homology-like domain, family A, member 1
Hs.268557	pleckstrin homology-like domain, family A, member 3
Hs.494406	sema domain, immunoglobulin domain (Ig), transmembrane domain (TM) and short cytoplasmic domain, (semaphorin) 4D
Hs.595276	signal transducer and activator of transcription 5B
Hs.479754	similar to Mast/stem cell growth factor receptor precursor (SCFR) (Proto-oncogene tyrosine-protein kinase Kit) (c-kit) (CD117 antigen); v-kit Hardy-Zuckerman 4 feline sarcoma
Hs.68061	sphingosine kinase 1
Hs.164226	thrombospondin 1
Hs.519033	toll-like receptor 2
Hs.29344	toll-like receptor adaptor molecule 1
Hs.592317	transforming growth factor, beta 3
Hs.129708	tumor necrosis factor (ligand) superfamily, member 14
Hs.212680	tumor necrosis factor receptor superfamily, member 18
Hs.73793	vascular endothelial growth factor A

Table S1. Genes associated with apoptosis unique to IPF from published disease list (Emblom-Callahan, 2010) analyzed by DAVID.

Unigene	Gene Name	Fold Change
	PREDICTED: similar to pleckstrin homology domain containing, family M (with RUN domain) member 1; adapter protein 162 [Source:RefSeq_peptide;Acc:XP_496237]	2.8779964
Hs.133444	DNA excision repair protein ERCC-6 (Cockayne syndrome protein CSB). [Source:Uniprot/SWISSPROT;Acc:Q03468]	2.816706
Hs.515079	Leucine-rich alpha-2-glycoprotein precursor (LRG). [Source:Uniprot/SWISSPROT;Acc:P02750]	3.3185902
Hs.25333	Interleukin-1 receptor, type II precursor (IL-1R-2) (IL-1R-beta) (Antigen CDw121b). [Source:Uniprot/SWISSPROT;Acc:P27930]	4.9874682
Hs.631504	Ras association domain family 2. [Source:Uniprot/SWISSPROT;Acc:P50749]	2.8310983
Hs.523360	Type I inositol-1,4,5-trisphosphate 5-phosphatase (EC 3.1.3.56) (5PTase). [Source:Uniprot/SWISSPROT;Acc:Q14642]	2.8955169
Hs.505874	TANK-binding kinase 1 [Source:RefSeq_peptide;Acc:NP_037386]	2.7836509
Hs.632587	PREDICTED: hypothetical protein XP_374786 [Source:RefSeq_peptide;Acc:XP_374786]	4.0108566
Hs.465490	RNA polymerase II subunit A C-terminal domain phosphatase (EC 3.1.3.16) (TFIIF-associating CTD phosphatase). [Source:Uniprot/SWISSPROT;Acc:Q9Y5B0]	3.0608847
Hs.550529	Similar to Caspase recruitment domain protein 14 (CARD-containing MAGUK protein 2) (Carma 2)	3.77252
Hs.1547	Inward rectifier potassium channel 2 (Potassium channel, inwardly rectifying, subfamily J, member 2) (Inward rectifier K(+) channel Kir2.1) (Cardiac inward rectifier potassium channel) (IRK1). [Source:Uniprot/SWISSPROT;Acc:P63252]	5.736548
Hs.721744	Beta-defensin 2 precursor (BD-2) (hBD-2) (Defensin, beta 2) (Skin-antimicrobial peptide 1) (SAP1). [Source:Uniprot/SWISSPROT;Acc:O15263]	2.8936
Hs.195080	Endothelin-converting enzyme 1 (EC 3.4.24.71) (ECE-1). [Source:Uniprot/SWISSPROT;Acc:P42892]	4.403086
Hs.1466	Glycerol kinase (EC 2.7.1.30) (ATP:glycerol 3-phosphotransferase) (Glycerokinase) (GK). [Source:Uniprot/SWISSPROT;Acc:P32189]	4.3848033
	PREDICTED: hypothetical protein from EUROIMAGE 588495 [Source:RefSeq_peptide;Acc:XP_051862]	3.3974285
Hs.524517	Granulocyte colony stimulating factor receptor precursor (G-CSF-R) (CD114 antigen). [Source:Uniprot/SWISSPROT;Acc:Q99062]	3.419708
Hs.480116	WD repeat and FYVE domain containing 3 isoform 2 [Source:RefSeq_peptide;Acc:NP_848698]	2.7759883
Hs.21239	Rabphilin-3A (Exophilin 1). [Source:Uniprot/SWISSPROT;Acc:Q9Y2J0]	3.1234498
Hs.654671	phosphatidylglycerophosphate synthase [Source:RefSeq_peptide;Acc:NP_077733]	4.092493

Hs.497951	-	3.128386
	Solute carrier organic anion transporter family, member 4A1 (Solute carrier family 21, member 12) (Sodium-independent organic anion transporter E) (Organic anion transporting polypeptide E) (OATP-E) (Colon organic anion transporter) (Organic anion transpo	6.1000385
Hs.33368	multiple C2-domains with two transmembrane regions 2 [Source:RefSeq_peptide;Acc:NP_060819]	4.6865845
Hs.531619	EGF-like module containing mucin-like hormone receptor-like 2 precursor (EGF-like module EMR2). [Source:Uniprot/SWISSPROT;Acc:Q9UHX3]	3.3042023
Hs.355753	putative lysophosphatidic acid acyltransferase [Source:RefSeq_peptide;Acc:NP_848934]	3.2707975
	Pro-neuregulin-1 precursor (Pro-NRG1) [Contains: Neuregulin-1 (Neu differentiation factor) (Heregulin) (HRG) (Breast cancer cell differentiation factor p45) (Acetylcholine receptor inducing activity) (ARIA) (Sensory and motor neuron-derived factor) (Glial	3.1475573
Hs.594861	Non-protein coding transcript	4.2559247
Hs.255479	Adenosine deaminase (EC 3.5.4.4) (Adenosine aminohydrolase). [Source:Uniprot/SWISSPROT;Acc:P00813]	5.7053604
Hs.559459	-	4.3150253
Hs.654758	Heparin sulfate N-deacetylase/N-sulfotransferase (EC 2.8.2.-) (N-HSST) (N-heparin sulfate sulfotransferase) (Glucosaminyl N-deacetylase/N- sulfotransferase). [Source:Uniprot/SWISSPROT;Acc:P52849]	3.2994452
Hs.276925	GTP-binding protein 1 (G-protein 1) (GP-1) (GP1). [Source:Uniprot/SWISSPROT;Acc:O00178]	4.69132
Hs.312579	Matrix metalloproteinase-25 precursor (EC 3.4.24.-) (MMP-25) (Membrane-type matrix metalloproteinase 6) (MT-MMP 6) (Membrane-type-6 matrix metalloproteinase) (MT6-MMP) (Leukolysin). [Source:Uniprot/SWISSPROT;Acc:Q9NPA2]	5.3867693
Hs.494406	Semaphorin 4D precursor (Leukocyte activation antigen CD100) (BB18) (A8) (GR3). [Source:Uniprot/SWISSPROT;Acc:Q92854]	3.7776742
Hs.232165	-	5.152434
Hs.567384	Proline-serine-threonine phosphatase-interacting protein 2. [Source:Uniprot/SWISSPROT;Acc:Q9H939]	8.4119
Hs.24309	S-acyl fatty acid synthase thioesterase, medium chain (EC 3.1.2.14) (Thioesterase II) (Thioesterase domain containing protein 1). [Source:Uniprot/SWISSPROT;Acc:Q9NV23]	7.1182156
Hs.383403	Probable G-protein coupled receptor 97 precursor (G-protein coupled receptor PGR26). [Source:Uniprot/SWISSPROT;Acc:Q86Y34]	7.0811706

Table S2. Fold changes of significant genes upregulated in IPF fibroblasts in microarray analysis of Normal-F (n=3) and IPF-F (n=4) used in this study.

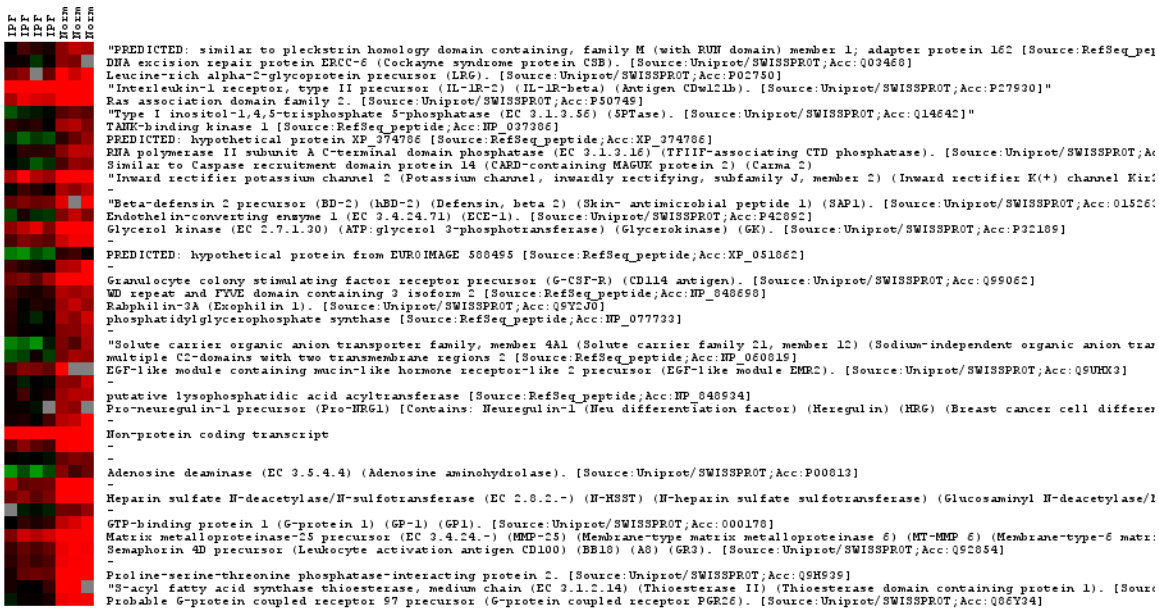

Figure S1. Heat map from microarray analysis qualitatively shows the significantly differentially regulated genes of IPF-F compared to N-F used in this study.

Unigene	Gene Name	Fold Change
Hs.183075	Sarcoplasmic/endoplasmic reticulum calcium ATPase 1 (EC 3.6.3.8) (Calcium pump 1) (SERCA1) (SR Ca(2+)-ATPase 1) (Calcium-transporting ATPase sarcoplasmic reticulum type, fast twitch skeletal muscle isoform) (Endoplasmic reticulum class 1/2 Ca(2+) ATPase).	1.0654612
	Sarcoplasmic/endoplasmic reticulum calcium ATPase 2 (EC 3.6.3.8) (Calcium pump 2) (SERCA2) (SR Ca(2+)-ATPase 2) (Calcium-transporting ATPase sarcoplasmic reticulum type, slow twitch skeletal muscle isoform) (Endoplasmic reticulum class 1/2 Ca(2+) ATPase).	1.7819971
Hs.414795	Plasminogen activator inhibitor-1 precursor (PAI-1) (Endothelial plasminogen activator inhibitor) (PAI). [Source:Uniprot/SWISSPROT;Acc:P05121]	0.551151
Hs.510334	Plasma serine protease inhibitor precursor (PCI) (Protein C inhibitor) (Plasminogen activator inhibitor-3) (PAI3) (Acrosomal serine protease inhibitor). [Source:Uniprot/SWISSPROT;Acc:P05154]	1.4532037
Hs.594481	Plasminogen activator inhibitor-2 precursor (PAI-2) (Placental plasminogen activator inhibitor) (Monocyte Arg-serpin) (Urokinase inhibitor). [Source:Uniprot/SWISSPROT;Acc:P05120]	3.1840246
Hs.597664	Inhibitor of nuclear factor kappa B kinase beta subunit (EC 2.7.1.37) (I-kappa-B-kinase beta) (IkBKB) (IKK-beta) (IKK-B) (I-kappa-B kinase 2) (IKK2) (Nuclear factor NF-kappa-B inhibitor kinase beta) (NFKBIKB). [Source:Uniprot/SWISSPROT;Acc:O14920]	1.9754843
Hs.618430	Nuclear factor NF-kappa-B p105 subunit (DNA-binding factor KBF1) (EBP- 1) [Contains: Nuclear factor NF-kappa-B p50 subunit]. [Source:Uniprot/SWISSPROT;Acc:P19838]	1.9232075
Hs.73090	Nuclear factor NF-kappa-B p100/p49 subunits (DNA-binding factor KBF2) (H2TF1) (Lymphocyte translocation chromosome 10) (Oncogene Lyt-10) (Lyt10) [Contains: Nuclear factor NF-kappa-B p52 subunit]. [Source:Uniprot/SWISSPROT;Acc:Q00653]	2.385966
Hs.502875	Transcription factor p65 (Nuclear factor NF-kappa-B p65 subunit). [Source:Uniprot/SWISSPROT;Acc:Q04206]	0.92398894
Hs.9731	NF-kappaB inhibitor beta (NF-kappa-BIB) (I-kappa-B-beta) (IkappaBbeta) (IKB-beta) (IKB-B) (Thyroid receptor interacting protein 9) (TR- interacting protein 9). [Source:Uniprot/SWISSPROT;Acc:Q15653]	1.5068345
Hs.618430	Nuclear factor NF-kappa-B p105 subunit (DNA-binding factor KBF1) (EBP- 1) [Contains: Nuclear factor NF-kappa-B p50 subunit]. [Source:Uniprot/SWISSPROT;Acc:P19838]	1.9232075

Table S3. Highlights of fold changes in genes of interest upregulated in IPF fibroblasts not statistically significant due to sample size from microarray analysis of Normal-F (n=3) and IPF-F (n=4) used in this study.

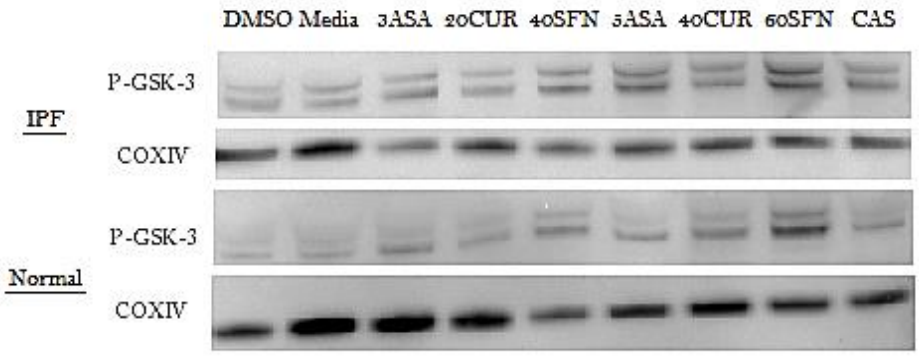

Figure S2. Western blot analysis of phosphorylated GSK3 protein expression in IPF-F and N-F following sublethal concentrations of Aspirin (3mM), Curcumin (20µM), and Sulforaphane (40µM) compared to lethal concentrations (5mM, 40µM, and 60µM, respectively) and CAS. COX-IV was used as loading control.

REFERENCES

Aggarwal BB, Shisodia S, Takada Y, Banerjee S, Newman RA, Bueso-Ramos CE, et al. Curcumin suppresses the paclitaxel-induced nuclear factor-kappaB pathway in breast cancer cells and inhibits lung metastasis of human breast cancer in nude mice. 2005; 11:7490-8.

Aggarwal BB, Sung B. Pharmacological basis for the role of curcumin in chronic diseases: an age-old spice with modern targets. Trends Pharmacol Sci. 2009: 30(2): 85-94.

Aggarwal S, Takada Y, Singh S, Myers JN, Aggarwal BB. Inhibition of growth and survival of human head and neck squamous carcinoma cells by curcumin via modulation of nuclear factor-kappB signaling. 2004;111-697-92.

Ambrosone CB, McCann, SE, Freudenheim JL, Marhsall JR, Zhang Y, Shields PG. Breast cancer risk in premenopausal women is inversely associated with consumption of broccoli, a soruce of isothiocyanates, but is not modified by GST genoype. J Nutr. 2004; 134:1134-1138.

Azuma A, Nukiwa T, Tsuboi E, et al. Double-blind, placebo-controlled trial of Pirfenidone in patients with idiopathic pulmonary fibrosis. Am J Respir Crit Care Med.

Bardales RH, Xie SS Schaefer RF, Hsu SM. Apoptosis is a major pathway responsible for the resolution of type II pneumocytes in acute lung injury. Am J Pathol. 1996; 149(3):845-852.

Bharti AC, Shishodia S, Reuben JM, Weber D, Alexanian R, Raj-Vadhan S, et al. Nuclear factor-kappaB and STAT3 are constitutively active in CD138+ cells dereived from multiple myeloma patients, and suppression of these transcription factor leads to apoptosis. 2004-103:3175-84.

Bouros D, Antoniou KM. Current and future therapeutic approaches in idiopathic pulmonary fibrosis. Eur Respir J. 2005; 26:693–702.

Bringardener BD, Baran CP, Eubank TD, Marsh CB. The Role of Inflammation in the Pathogenesis of Idiopathic Pulmonary Fibrosis. Antioxidants & Redox Signaling. 2008; 10(2):287–301.

Bush JA, Cheung Jr KJ, Li G. Curucmin induces apoptosis in human melanoma cells through a Fas receptor/caspase-8 pathway independent of p53. 2001; 271:305-14.

Chang W, Wei K, Jacobs S, Upadhyay D, Weill D, Rosen G. SPARC Suppresses Apoptosis of Idiopathic Pulmonary Fibrosis Fibroblasts through Constitutive Activation of β-Catenin. 2010; 285(11):8196-8206.

Chen A, Zheng S. Curcumin inhibits connective tissue growth factor gene expression in activated hepatic stellate cells in vitro by blocking NF-kappaB and ERK signalling. British journal of pharmacology. 2008: 153(3): 557-567.

Chen WC, Lai YA, Lin YC, Ma JW, Huang LF, Yang NS, Ho CT, Kuo SC, Way TD. Curcumin suppresses doxorubicin-induced epithelial-mesenchymal transition via the inhibition of TGF-beta and PI3K/AKT signaling pathways in triple-negative breast cancer cells. Journal of agricultural and food chemistry. 2013: 61(48): 11817-11824.

Das L, Vinayak M. Long-term effect of curcumin down-regulates expression of tumor necrosis factor-alpha and interleukin-6 via modulation of E26 transformation-specific protein and nuclear factor-kappaB transcription factors in livers of lymphoma bearing mice. Leukemia & lymphoma. 2014.

Deeb D, Jiang H, Gao X, Al-Holou S, Danyluk AL, Dulchavsky SA, et al. Curcumin sensitizes human prostate cancer cells to tumor necrosis factor-related apoptosis-inducing ligand/Apo2L-induced apoptosis by suppressing nuclear factor-kappB via inhibition of the prosurvival Akt signaling pathway. 2007; 321:16-25.

Degterev A, Yuan J. Expansion and evolution of cell death programmes. Nat. Rev. Mol. Cell Biol. 2008; 9(5):378–90.

Dunsmore SE, Shapiro SD. The bone marrow leaves its scar: new concepts in pulmonary fibrosis. J Clin Invest. 2004; 113:190-182.

Emblom-Callahan MC, Chhina MK, Shlobin OA, Ahmad S, Reese ES, Iyer EPR, Cox DN, Brenner R, Burton NA, Grant GM, Nathan SD. Genomic Phenotype of Non-cultured Pulmonary Fibroblasts in Idiopathic Pulmonary Fibrosis. Genomics 2010: In Press.

Fattman CL. Apoptosis in pulmonary fibrosis: too much or not enough? Antioxid Redox Signal. 2008; 10(2): 379-85.

Fowke JH, Chung FL, Jin F, Qi D, Cai Q, Conaway C, Cheng JR, Shu XO, Gao YT, Zheng W. Urinary isothiocyanate levels, brassica, and human breast cancer. Cancer Res. 2003; 63;3980-86.

Fuchs Y, Steller H. Programmed cell death in animal development and disease. Cell. 2011; 147(4):742–58.

Gao X, Deeb D, Jiang H, Liu YB, Dulchavsky SA, Gautam SC. Curcumin differentially sensitizes malignant glioma cells to TRAIL/Apo2L-mediated apoptosis through activation of procaspases and release of cytochrome c from mitochondira. 2005; 5:39-48.

Gilani SR, Vuga U, Lindell KO, et al. CD28 down regulation on circulating CD4 T cells is associated with poor prognoses of patients with idiopathic pulmonary fibrosis. PLoS One. 2010; 5:e8959.

Giovannucci E, Rimm EB, Lui Y, Stampfer MJ, Willett WC. A prospective study of cruciferous vegetables and prostate cancer. Cancer Epidomeiol Biomarkers Prev. 2003; 12:1403-1409.

Gotoh I, Adachi M, Nishida E. Indentification and characterization of a novel MAP kinase kinase kinase, MLTK. J Biol Chem. 2001; 276:4276-4286.

Gotoh Y, Nishida E. Activation mechanism and function of the MAP kinase cascade. Mol Repro Dev. 1995; 42:486-492.

Gross TG, Hunninghake GW. Idiopathic pulmonary fibrosis. N Engl J Med. 2001; 245:517-525.

Gupta SC, Sung B, Kim JH, Prasad S, Li S, Aggarwal BB. Multitargeting by turmeric, the golden spice: From kitchen to clinic. Molecular nutrition & food research 2013: 57(9): 1510-1528.

Hashimoto N, Jin H, Lui T, Chensue SW, Phan SH. Bone marrow-derived progenitor cells in pulmonary fibrosis. J Clin Invest. 2004; 113:243-252.

Hojo S, Fujita J, Yamadori I, Kamei T, Yoshinouchi T, Ohtsuki Y, Okada H, Bandoh S, Yamaji Y, Takahara J, Fukui T, Kinoshita M. Heterogeneous point mutations of the p53 gene in pulmonary fibrosis. Eur Respir J. 1998;12(6):1404-8.

Hua Y, Dolence J, Ramanan S, Ren J, Nair S. Bisdemethoxycurcumin inhibits PDGF-induced vascular smooth muscle cell motility and proliferation. Molecular nutrition & food research. 2013: 57(9): 1611-1618.

Jee SH, Shen SC, Tseng CR, Chiu HC, Kuo ML. Curcumin induces a p53-dependent apoptosis in human basal cell carcinoma cells. 1998; 111:656-61.

Joseph, S. A Comprehensive Clinical Evaluation of 20,000 Persian Gulf War Veterans. Military Medicine. 1997; 162(3):149-155.

Jutooru I, Chadalapaka G, Lei P, Safe S. Inhibition of NFKβ and Pancreatic Cancer Cell and Tumor Growth by Curcumin is Dependent on Specificity Protein Down-regulation. J Biol Chem. 2010; 285(33):25332-44.

Karmakar S, Banik NL, Patel SJ, Ray SK. Curcumin activated both receptor-mediated and mitochondria-mediated proteolytic pathways for apoptosis in human glioblastoma T98G cells. 2006; 407:53-8.

Kaufmann T, Strasser A, Jost PJ. Fas death receptor signalling: roles of Bid and XIAP. Cell Death Differ. 2012; 19(1):42–50.

Kolch, W. Coordinating ERK/MAPK signaling through scaffolds and inhibitors. Nat Rev Mol Cell Biol. 2005; 6:827-837.

Kurokawa M, Kornbluth S. Caspases and kinases in a death grip. Cell. 2009;138(5):838–54.

Lev-Ari S, Strier L, Kazanov D, Elkayam O, Lichtenberg D, Caspi D, et al. Curcumin synergistically potentiates the growth-inhibitory and pro-apoptotic effects of celecoxib in osteoarthritis synovial adherent cells. 2006; 45:171-7.

Lev-Ari S, Zinger H, Kazanov D, Yoma D, Ben-Yosef R, Starr A, et al. Curcumin synergistically potentiates the growth inhibitory and pro-apoptotic effects of celecoxib in pancreatic adenocarcinoma cells. 2005; 59.

Lev-Ari Strier L, Kazanov D, Madar-Shapiro L, Dvory-Sobol H, Pinchuk I, et al. Celecoxib and curcumin synergistically inhibit the growth of colorectal cancer cells. 2005; 11:6738-44.

Li L, Aggarwal BB, Shishodia S, Abbruzzese J, Kurzrock R. Nuclear factor-kappaB and IkappaB kinase are constitutively active in human pancreatic cancer cells, and their down-regualtion by curcumin (diferuloylmethane) is associated with the suppression of proliferation and the induction of apoptosis. 2004; 101:2351-62.

Lin YL, Lin CY, Chi CW, Huang YT. Study on antifibrotic effects of curcumin in rat hepatic stellate cells. Phytother Res. 2009: 23(7): 927-932.

Liu CA, Wan MJ, Chi CW, Wu CW, Chen JY. Rho/THotekin-mediated NF-kappaB activation confers resistance to apoptosis. 2004; 23:8731-42.

Lond SJ, Yuan JM, Chung FL, Gao YT, Coetzee GA, Ross RK, Yu MC. Isothiocyanates, glutathione S-transferase M1 and T2 polymorphisms and lung-cancer risk: a prospective study of men in Shanghai, China. Lancet. 2000; 356:724-729.

Lurton JM, Trejo T, Narayanan AS. Pirfenidone inhibits the stimulatory effects of profibrotic cytokines of human lung fibroblasts in vitro. Am J Respir Crit Care Med. 1996; 153:A403.

MacGillivray, MK, Cruz TF, McCulloch, CA. The recruitment of the interleukin-1 receptor-associate kinase (IRAK) into focal adhesion complexes is require for IL-1beta-indecued ERK activation. 2000; 275:23509-15.

Mapel DW1, Hunt WC, Utton R, Baumgartner KB, Samet JM, Coultas DB. Idiopathic pulmonary fibrosis: survival in population based and hospital based cohorts. Thorax. 1998; 53(6):469-76.

Marin YE, Wall BA, Wang S, Namkoong J, Martino JJ, Suh J, et al. Curcumin downregualtes the constituve activity of NF-kappaB and induces apoptosis in novel mouse melanoma cells. 2007; 17:274-83.

Moeller A, Gilpin SE, Ask K, et al. Circulating fibrocytes are an indicator of poor prognosis in idiopathic pulmonary fibrosis. Am J Respir Crit Care Med. 2009; 179:588–594.

Moragoda L, Jaszewski R, Manjumdar AP. Curcumin induced modulation of cell cycle and apoptosis in gastric and colon cancer cells. 2001; 21:873-8.

Mukhopadhyay A, Bueso-Ramos C, Chatterjee D, Pantazis P, Aggarwal BB. Curcumin downregulates cell survival mechanisms in human prostate cancer cell lines. 2001; 20:7597-609.

Pfaffl, M.W. A new mathematical model for relative quantification in real-time RT–PCR. Nucleic Acids Res. 2001; 29:e45.

Phillips RJ, Brudick MD, Hong K, et al. Circulating fibrocytes traffic to the lungs in response to CXCL12 and mediate fibrosis. J Clin Invest. 2004; 114:438-446.

Pradelli LA, Bénéteau M, Ricci JE. Mitochondrial control of caspase-dependent and -independent cell death. Cell. Mol. Life Sci. 2010;67(10):1589–97.

Raghu G, Collard HR, Egan JJ, Martinez FJ, Behr J, Brown KK, Colby TV, Cordier J-F, Flaherty KR, Lasky JA, et al.. An official ATS/ERS/JRS/ALAT statement: idiopathic pulmonary fibrosis: evidence-based guidelines for diagnosis and management. Am J Respir Crit Care Med 2011;183:788–824.

Raghu G, Weycker D, Edelsherg J, Bradford WZ, Oste G. Incidence and prevalenace of pulmonary fibrosis deaths in the United States, 1979-1991; an analysis of multiple-cause mortality data. Am J Respir Crit Care Med. 2006; 174(9):810-816.

Ramachandran C, Rodriguez S, Ramachandran R, Raveendran Nair PK, Fonseca H, Khatib Z, et al. Expression profiles of apoptotic genes induced by curcumin in human breast cancer and mammary epithelial cell lines. 2005; 25:3293-302.

Ramos, C., M. Montano, et al. Fibroblasts from idiopathic pulmonary fibrosis and normal lungs differ in growth rate, apoptosis, and tissue inhibitor of metalloproteinases expression. Am J Respir Cell Mol Biol. 2001; 24(5): 591-8.

Ravindran J, Prasad S, Aggarwal B. Curcumin and Cancer Cells: How many ways can curry kill tumor cells selectively? American Association of Pharmaceutical Scientists. 2009;11(3):495-510.

Richards TJ, Kaminski N, Baribaud F, Flavin S, Brodmerkel C, Horowitz D, et al. Peripheral blood proteins predict mortality in idiopathic pulmonary fibrosis. Am J Respir Crit Care Med. 2012; 185:67–76.

Rosas IO, Richards TJ, Konishi K, et al. MMP1 and MMP7 as potential peripheral blood biomarkers in idiopathic pulmonary fibrosis. PLoS Med. 2008; 5:e93.

Rose C, Abraham J, Harkins D, et al. Overview and Recommendations for Medical Screening and Diagnostic Evaluation for Postdeployment Lung Disease in Returning US Warfighters. Journal of Occupational and Environmental Medicine. 2012; 54(6):746–751.

Salmeron A, Ahmad TB, Charlie, GW, Pappin D, Narshimhan, RP, Ley SC. Activation of MEK-1 and SEK-1 by Tpl-2 proto-oncoprotein, a novel MP kinase kinase kinase. Embo J. 1996; 15:817-826.

Schwartz DA, Dlemers RA, Galvin JR, et al. Determinatnts of survival in idiopathic pulmonary fibrosis. Am J Respir. Crit Care Med. 1994; 149:450-454.

Selman M. From anti-inflammatory drugs through antifibrotic agents to lung transportation. A long road of research, clinical attempts, and failures in treatment of idiopathic pulmonary fibrosis. Chest. 2002; 123:749-761.

Sen, S sharma H, Singh N. Curcumin enhances Vinorelbine mediated apopsosi in NSCLC cells by the mitochondrial pathway. 2005; 331:1245-52.

Seo JA, Kim B, Dhanasekaran DN, Tsang BK, Song YS. Curcumin induces apoptosis by inhibiting sarco/endoplasmic reticulum Ca(2+) ATPase activity in ovarian cancer cells. 2016. Cancer Lett. 2016; 371(1):30-7.

Seow A, Yuan JM, Sun CL, Van Den Berg D, Lee HP, Yu MC. Dietary isothiocyanates, glutathione s-transferase polymorphisms and colorectal cancer risk in he Singapore Chinese Health Study. Carcinogensis. 2002; 23:2055-61.

Shishodia S, amin HM, Lai R, Aggarwal BB. Curcumin (diferuloylmehane) inhibits constitutive NF-kappaB activation, induces G1/S arrest, suppresses proliferation, and induces apoptosis in mantle cell lymphoma. 2005; 70:700-13.

Shishodia S. Molecular mechanisms of curcumin action: gene expression. BioFactors (Oxford, England). 2013: 39(1): 37-55.

Simone NL, Soule BL, Gerber L, et al. Oral pirfenidone in patients with chronic fibrosis resulting from radiotherapy: a pilot study. Radiation Onc. 2007; 2(19).

Smith MR, Gangireddy SR, Narala VR, Hogaboam CM, Standiford TJ, Christensen PJ, Kondapi AK, Reddy RC. Curcumin inhibits fibrosis-related effects in IPF fibroblasts and in mice following bleomycin-induced lung injury. American journal of physiology. 2010: 298(5): L616-625.

Sokai A, Handa T, Tanizawa K, et al. Matrix metalloproteinase-10: a novel biomarker for idiopathic pulmonary fibrosis. Respiratory Research. 2015; 16:120.

Sperandio S, de Belle I, Bredesen DE. An alternative, nonapoptotic form of programmed cell death. Proceedings of the National Academy of Sciences of the United States of America. 2000; 97(26):14376-14381.

Sptiz MR, Durphorne CM, Detry MA, Pillow PC, Amos CI, Lei L, De Andrade M, Gu X, Hong WK, Wu X. Dietary intake of isothiocyanates: evidence of a join effect with glutathione S-transferase polymorphisms in lung cancer risk. Cancer Epidemiol. Biomarkers Prev. 2000; 9:1017-20.

Syng-Ai C, Kumari AL, Khar A. Effect of curcumin on normal and tumor cells: role of glutathione and bcl-2. Mol Cancer Ther 2004: 3(9): 1101-1108.

Thannickal VJ, Flaherty KR, Hyzyrcl RC, Lynch JP. Emerging drugs for idiopathic pulmonary fibrosis. Exp Opin Emerging Drugs. 2005; 10(4):707-727.

Thannickal VJ, Horowitz JC. "Evolving concepts of apoptosis in idiopathic pulmonary fibrosis." Proc Am Thorac Soc. 2006; 3(4): 350-6.

Uhal BD, Joshi I, Hughes WF, Ramos C, Pardo A, Selman M. Alveolar epithelial cell death adjacent to underlying myofibroblasts in advacnced fibrotic human lung. Am J Physiol. 1998;275:L1192-L1199.

Van Breda SGJ, de Kok TMCM, van Delft JHM. Mechanisms of colorectal and lung cancer prevention by vegetables: a genomic approach. The Journal of Nutritional Biochemistry. 2008;19:139–157.

Van Oortegem K, Wallaert B, Marquette CH, et al.Determinants of response to immunosuppressive therapy in idiopathic pulmonary fibrosis. Eur Respir J 1994; 7:1950–1957.

Walter N, Harold RH, Collarad HR, King TE. Current perspectives on treatment of idiopathic pulmonary fibrosis. Proc Am Throac Soc. 2006; 3:330-338.

Wang LI, Giovannucci El, Hunter D, Neurber D, Su L, and Christiani DC. Dietary intake of cruciferous vegetables, glutathione S-transferase (GST) polymorphisms and lung cancer risk in a Caucasian population. Cancer Causes Control. 2004; 15:977-985.

Wang, J, Chun HJ, Wong W, Spencer DM, Lenardo MJ. Caspase-10 is an initiator caspase in death receptor signaling. 2001; 98:13884-8.

Well AU, Hogaboam CM. Update in diffuse parenchymal lung disease. Am J Repsir Crit Care Med. 2007;175:(7)655-660.

Whal H, Tan L, Griffith K, Choi M, Lui JR. Curcumin enhances Apo2L/TRAIL-induced apoptosis in chemoresistant ovarian cancer cells 2007;105:104-12.

Willis BC, DuBois RM, Brok Z. Epithelial origin of myofibroblasts during fibrosis in the lung. Proc Am Thorac Soc. 2006; 3:377-382.

Wu M, Gordon RE, Herbert R, Padilla M, Moline J, Mendelson D, Litle V, Travis WD, Gil J. Case report: Lung disease in World Trade Center responders exposed to dust and smoke: carbon nanotubes found in the lungs of World Trade Center patients and dust samples. Environ Health Perspect. 2010; 118(4):499-504

Yoon S, Seger R. The extracellular signal-regulated kinase: multiple subtrastes regulate diverse cellular functions. Growth factors. 2006; 24:21-44.

Zhang D, Huang C, Yang C, Liu RJ, Wang J, Niu J, Bromme D. Antifibrotic effects of curcumin are associated with overexpression of cathepsins K and L in bleomycin treated mice and human fibroblasts. Respiratory research. 2011: 12: 154.

Zhao B, Seow A, Lee EJ, Poh WT, The M, Eng P, Wang YT, Tan WC, Yu MC, Lee HP. Dietary isothiocyanates, glutathione S-transferases –M1, -T1 polymorphisms and lung cancer risk among Chinese women in Singapore. Cancer Epidemiol. Biomarkers Prev. 2001;10:1063-1067.

Zisman DA, Lynch, JP, Toews GB, et al. Cyclophosphamide in treatment of idiopathic pulmonary fibrosis: a prospective study in patients who failed to respond to corticosteroids. Chest. 2000; 117(6):1619-1626.

BIOGRAPHY

Sarah Bui graduated from Battlefield High School, Haymarket, Virginia, in 2011. She received her Bachelor of Science degree in Biology from Virginia Commonwealth University, Richmond, Virginia in 2013.